PENSOFT
SENCKENBERG world of biodiversity
Leibniz Association

Systematics and phylogeny of the Andean genera *Konradus* Chani-Posse & Ramírez-Salamanca and *Yuracarus* gen. nov. (Coleoptera: Staphylinidae)

Mariana Raquel Chani-Posse[1], Maryzender Erceliz Rodríguez-Melgarejo[1,2,4], José Manuel Ramírez-Salamanca[1,3]

1 *Laboratorio de Entomología, Instituto Argentino de Investigaciones de las Zonas Áridas (IADIZA, CCT CONICET, Mendoza), Casilla de Correo 507, 5500 Mendoza, Argentina*

2 *Programa de Doctorado en Ciencias Naturales, Universidad Nacional de La Plata, Buenos Aires, Argentina*

3 *Laboratorio de Entomología de la Pontificia Universidad Javeriana, Bogotá, Colombia*

4 *Departamento de Entomología, Museo de Historia Natural de la Universidad Nacional Mayor de San Marcos, Lima, Perú*

https://zoobank.org/4DE64D12-8127-4F6C-95C0-14CD6FFF21E5

Corresponding author: Mariana Chani-Posse (mchani@mendoza-conicet.gob.ar)

Received 14 February 2025
Accepted 12 May 2025
Published 21 July 2025

Academic Editor Vinicius S. Ferreira

Citation: Chani-Posse MR, Rodríguez-Melgarejo ME, Ramírez-Salamanca JM (2025) Systematics and phylogeny of the Andean genera *Konradus* Chani-Posse & Ramírez-Salamanca and *Yuracarus* **gen. nov.** (Coleoptera: Staphylinidae). Arthropod Systematics & Phylogeny 83: 331–352. https://doi.org/10.3897/asp.83.e150304

Abstract

Konradus Chani-Posse & Ramírez-Salamanca, 2020 was originally described as a monotypic genus from the tropical Andes of Ecuador. However, a re-examination of type material from species previously classified under the genus *Philonthus Stephens*, 1829, along with additional, previously unstudied specimens collected from high-altitude regions (above 2000 m) in the Andes of Ecuador, Peru, and Bolivia, prompted a more comprehensive reassessment of the genus. This study presents a revision of *Konradus* and introduces *Yuracarus* **gen. nov.**, based on external morphology and male and female sexual characters. Two species previously considered "false *Philonthus*" (*Ph. actinus* Bernhauer, 1917 and *Ph. diamantinus* Bernhauer, 1917) are transferred to *Konradus* and *Yuracarus* **gen. nov.**, respectively: *K. actinus* (Bernhauer), **new comb**., and *Y. diamantinus* (Bernhauer), **new comb.** Additionally, two species from Peru are newly described within *Konradus*: *K. cuscensis* **sp. nov.** and *K. trescrucensis* **sp. nov.**, while three new species are described within *Yuracarus*: *Y. cosnipatensis* **sp. nov.**, *Y. napoensis* **sp. nov.**, and *Y. yunguensis* **sp. nov.** A key to species, diagnoses, descriptions and/or redescriptions, illustrations, a distributional map, and a phylogenetic analysis are included. Lectotypes are designated for *Philonthus actinus* Bernhauer and *Philonthus diamantinus* Bernhauer. Cladistic analysis confirms the monophyly of *Konradus* and *Yuracarus* within the Andean clade (AC) of Neotropical Philonthina and supports *Yuracarus* as a distinct genus. Both genera are part of a well-supported clade characterized by the presence of sub-bilobed and subtriangular protarsomeres 2 and 3, bearing discal setae on their ventral surface, as well as a horseshoe-shaped accessory sclerite associated with female tergum 10.

Keywords

Bolivia, Ecuador, morphology, new genus, Peru, Philonthina, Staphylininae, Tropical Andes

Copyright *Mariana Raquel Chani-Posse* et al.: This is an open access article distrixbuted under the terms of the Creative Commons Attribution License (CC BY 4.0), which permits unrestricted use, distribution, and reproduction in any medium, provided the original author and source are credited.

1. Introduction

Previous studies on Philonthina have consistently demonstrated the non-monophyly of the megadiverse and globally distributed genus *Philonthus* Stephens, 1829 (e.g., Smetana 1995; Chani-Posse et al. 2018a, 2018b). With over 1,300 species (Newton 2025), *Philonthus* remains a central challenge in establishing natural generic boundaries within the subtribe. Despite this, certain traits—such as the presence of protarsi with distally widened tarsomeres 1–4 bearing modified (adhesive) pale setae on their ventral surface—have consistently been identified as defining characters of *Philonthus* (Smetana 1995). However, this condition is not exclusive to *Philonthus* and is, in fact, widespread in Staphylinini (i.e., a plesiomorphic character). Moreover, the configuration of both the protarsomeres and the setae has been shown to be non-homologous between Holarctic *Philonthus* and many of its extra-Holarctic representatives, including "false" *Philonthus* species within the Neotropical lineage of Philonthina (NL hereafter) (Chani-Posse and Ramírez-Salamanca 2020a). Among these, two species—*Ph. actinus* Bernhauer, 1917 and *Ph. diamantinus* Bernhauer, 1917—were originally described from the Tropical Andes of Bolivia (Bernhauer 1917). In contrast to other Neotropical species of Philonthina, these two species are characterized by their slender body shape, which includes both an elongate head and pronotum, as well as a habitus that is either entirely or predominantly metallic-colored. One of these, *Ph. diamantinus*, has previously been included in phylogenetic reconstructions of the NL, and consistently appeared in a monophylum alongside *Inesius callosipennis* (Scheerpeltz, 1960) (Ramírez-Salamanca et al. 2020), with both species closely related to one or the other of the monotypic genera *Konradus* Chani-Posse & Ramírez-Salamanca, 2020 (Chani-Posse and Ramírez-Salamanca 2020b) or *Delgadobius* Chani-Posse & Couturier, 2012 (Chani-Posse and Ramírez-Salamanca 2020a; Ramírez-Salamanca et al. 2020). Although all of these species exhibit metallic-colored elytra, *K. leehermani* Chani-Posse & Ramírez-Salamanca, 2020 and *Ph. diamantinus* are most easily distinguished from *Delgadobius amazonensis* Chani-Posse & Couturier, 2012 by their metallic coloration extending to the head and thorax, in addition to the elytra. In *K. leehermani*, the entire body is metallic-colored, while in *Ph. diamantinus*, the metallic coloration is limited to the head, thorax, and elytra as in the species of *Inesius* (Ramírez-Salamanca et al. 2020). On the other hand, both *K. leehermani* and *Ph. diamantinus* also have scarcely punctate elytra, in contrast to those of *Delgadobius* and *Inesius*, whose species exhibit distinctly punctate elytra. As part of our ongoing study on the generic boundaries within the NL of Philonthina, we re-examined type material from the two aforementioned "false" *Philonthus* species, *Ph. actinus* and *Ph. diamantinus*, as well as additional non-type material from other collections. This led to their reclassification into the previously monotypic genus *Konradus* and the establishment of a new genus, *Yuracarus*. *Konradus* is currently known from a single species found in the Andes of Ecuador, at an elevation of approximately 2000 m above sea level. Similarly, both *Ph. actinus* and *Ph. diamantinus* were originally known only from one distinct locality at around 2000 m in Cochabamba, Bolivia (Newton 2025).

In addition to revising *Konradus*, describing the new genus *Yuracarus*, and reclassifying and redescribing *Ph. actinus* and *Ph. diamantinus*, we describe five new species based on recently examined material collected from high-altitude regions in the Andes of Ecuador, Peru, and Bolivia. Of these, two species are assigned to *Konradus*, and three to the newly established genus *Yuracarus*, which also includes *Ph. diamantinus*. Finally, we test the monophyly of both genera and explore their phylogenetic relationships within the Neotropical lineage of Philonthina.

2. Material and methods

2.1. Examination of material and terminology

The material studied was borrowed from the following depositories: **CNC** – Canadian National Collection, Ottawa, Canada (Adam Brunke, Patrice Bouchard) — **FMNH** – The Field Museum of Natural History, Chicago, USA (Maureen Turcatel, Alfred Newton, Margaret Thayer) — **MUSM** – Museo de Historia Natural, Universidad Nacional Mayor de San Marcos, Lima, Perú (Diana Silva, Gerardo Lamas) — **NHMUK** – The Natural History Museum, London, UK (Max Barclay).

Beetle specimens were examined using a Nikon SMZ 745 dissecting microscope. They were mostly examined as pinned dry specimens, but two of them were first relaxed in warm soapy water, rinsed, disarticulated and examined as wet preparations in ethanol. Techniques for the preparation and examination of male and female genitalia follow Smetana (1982). Habitus photograph was taken using a Canon 750D. SEM images were obtained by using a JSM-6610 system. Photographs and/or line drawings of sexual characters were made using a digital camera attached to the dissecting microscope, with line drawings traced from the photographs. Depositories of type material retain the copyright of the photographs. Measurements (given in millimeters) were made with an ocular micrometer. Overall body length was measured from the apex of the labrum to the apex of the abdomen. Other measurements were taken and abbreviated as follows:

HW Head capsule maximum width (measured at widest point);
HL Length of head capsule, from anterior margin of frontoclypeus to neck constriction (along midline);
Lp2L, **Lp3L** Length of second or third labial palpomere;
PW Pronotum maximum width;
PL Pronotum length along midline;
EL Eye length (seen from above);

TL Temple length (from the posterior margin of the eye to the nuchal groove; seen from above);
NW Neck width;
S1, **S5** Length of first or fifth (last) metatarsomere;
EtL Elytron length at side (straight line from humerus to apex; seen from above).

Terminology follows authors and criteria as stated in Chani-Posse and Ramírez-Salamanca (2020a, 2020b). Exact label data are cited for the type material, with separate labels enclosed in double quotation marks "" and separate lines within a label indicated by a slash /. Text in square brackets [] denotes explanatory or inferred information. All locality data were recorded from specimen labels, georeferenced by Google Earth (Google Inc.) and plotted onto a relief map derived from a digital elevation model using QGIS 3.10.0 (QGIS Development Team 2020). Handwriting on labels of type specimens were compared to the respective author's handwriting as shown by Horn et al. (1990).

During the preparation of this work, ChatGPT Open AI was used solely in order to improve language and readability. After this tool/service was used, the content was reviewed and edited as needed, and full responsibility for the content of the publication is taken by the authors herein.

2.2. Phylogenetic analysis

2.2.1. Outgroup and ingroup taxa

A total of twenty-three terminal units are included in the phylogenetic analysis. In addition to *Konradus leehermani*, the type species, this analysis includes the other three species recognized as *Konradus*, along with the four species belonging to the newly established genus *Yuracarus* **gen. nov.** Fifteen additional species are also included, representing genera (including type species* or species within the type species group) from Philonthina and its NL, with a focus on the Andean clade (AC hereafter) (Ramírez-Salamanca et al. 2024): *Belonuchus* Nordmann, 1837 [*B. haemorrhoidalis* (Fabricius, 1801)*], *Corisantis* Chani-Posse & Rodríguez-Melgarejo, 2024 [*Corisantis candens* (Erichson, 1840)*], *Carmenlyrus* Chani-Posse et al., 2022 [*C. thayerae* Chani-Posse et al., 2022*], *Chroaptomus* Sharp [*Ch. flagrans* (Erichson, 1840)*], *Delgadobius* Chani-Posse & Couturier, 2012 [monotypic: *D. amazonensis* Chani-Posse & Couturier, 2012*], *Inesius* Ramírez-Salamanca et al., 2020 [*I. callosipennis* (Scheerpeltz, 1960)*], *Leptopeltoides* Chani-Posse & Asenjo, 2013 [*Le. ecuatoriensis* Chani-Posse & Asenjo, 2013*], *Leptopeltus* Bernhauer, 1906 [*L. flavipennis* (Erichson, 1840)*], *Paederomimus* Sharp, 1885 [*P. contractus* Sharp, 1885], *Proxenobius* Seevers 1965 [monotypic: *Proxenobius borgmeieri* Seevers, 1965*], *Pseudochroaptomus* Chani-Posse et al., 2024 [monotypic: *Pse. ecuadoriensis* Chani-Posse et al., 2024*] and *Rhaegalius* Ramírez-Salamanca et al., 2020 [monotypic: *R. sophia* Ramírez-Salamanca et al., 2020*]. The latter was included in our analysis as representative of an AC subclade characterized by rectangular (i.e., flattened and transverse) protarsomeres, which also comprises the monotypic genus *Atopocentrum* Bernhauer (Rodríguez-Melgarejo et al., ms submitted). The "false" *Philonthus* species, *Ph. fulgipennides* Newton, 2017, was also included in representation of the *fulgipennides*-group within the AC. Following Chani-Posse et al. (2018a) and Chani-Posse and Ramírez-Salamanca (2020a), a representative of *Gabrius* Stephens, 1829 [*G. picipennis* (Mäklin, 1852)] was included due to its potential sister-group relationship with the NL and *Philonthus* Stephens, 1829 [*Ph. splendens* (Fabricius, 1792)*] was used to root the tree.

2.2.2. Characters

Sixty-seven morphological characters (see File S1) were coded and scored for the 23 terminal units, with their selection and definition following Chani-Posse and Ramírez-Salamanca (2020a, 2020b), Ramírez-Salamanca et al. (2020) and Chani-Posse and Rodríguez-Melgarejo (2024) based on their effectiveness in resolving relationships at the generic level within the NL of Philonthina and its AC. Fifty-two characters were chosen from external morphology and 15 from sexual characters. Among these, 17 characters (in parentheses) are parsimoniously uninformative. They were excluded from the analysis for the calculation of tree statistics but retained in the matrix to make them traceable in the tree as potential autapomorphic characters. All characters were treated as unordered (non-additive) and given equal weight. Ten characters from this list (*) are novel and illustrated herein.

1* Body, metallic coloration: **[0]** absent or limited to elytra; **[1]** limited to head, thorax and elytra (e.g., Fig. 1D); **[2]** entire body (i.e., head, thorax, elytra and abdomen) (e.g., Fig. 1A).
2 Antennal insertions (ai), position in relation to frontoclypeus and eye (see Chani-Posse 2014a): **[0]** ai situated at the anterior margin of frontoclypeus, i.e., anterior margin of antennal cavity touching the anterior margin of frontoclypeus (fig. 3E); **[1]** ai situated closer to frontoclypeus than to eye (fig. 3D); **[2]** ai situated at equal distance or closer to eye (fig. 11D).
3 Antennal insertions (ai), position (see Chani-Posse 2014a): **[0]** ai situated in fossae (fig. 3E); **[1]** ai not situated in fossae (fig. 3A–D).
4 Antennae, antennomeres 4–10, apical margin, shape: **[0]** concave to truncate; **[1]** distinctly convex.
5 Antennae, antennomere 5, shape: **[0]** elongate; **[1]** quadrate.
(6) Sexual dimorphism, frontoclypeus, emargination: **[0]** absent (i.e., both male and female without emargination); **[1]** present (emarginate in males) (Chani-Posse 2014a: fig. 11D).
7 Eyes, relative length to that of tempora: **[0]** subequal; **[1]** eyes distinctly longer than tempora; **[2]** eyes distinctly shorter than tempora.

8* Head, eye shape: **[0]** not protruding; **[1]** protruding (Fig. 2A–F).

9 Head shape, maximum width: **[0]** close to or at its anterior margin; **[1]** at its halfway between the anterior and posterior margin; **[2]** at or close to the posterior margin.

(10) Head, anterior angles next to eye margin: **[0]** without a distinct border; **[1]** with a distinct border (Chani-Posse et al. 2022: fig. 5).

11* Head, posterior angles: **[0]** almost obsolete (Fig. 2A–C); **[1]** distinct, not obsolete (Fig. 2D–F).

12 Head, postmandibular ridge: **[0]** absent; **[1]** present (Fig. 3A).

13 Head, distance between antennal insertions relative to shortest distance between anterior margin of eye to antennal insertion: **[0]** 2× or more; **[1]** distinctly less than 2×.

14 Head, labrum shape: **[0]** transverse; **[1]** subconical (Chani-Posse and Rodríguez-Melgarejo 2024: fig. 1B).

15 Head, ventral surface, microsculpture: **[0]** distinct (i.e., punctate near gular sutures); **[1]** not distinct.

16 Gular sutures, development from anterior margin of mentum to base of head: **[0]** not joined; **[1]** joined halfway; **[2]** joined rather close to base of head.

17 Labial palpus, relative length of palpomeres 3 (p3, apical) and 2 (p2, preapical) (p3/p2): **[0]** p3 distinctly shorter than p2; **[1]** p3 and p2 subequal in length; **[2]** p3 distinctly longer than p2.

18 Maxillary palpus, relative length of palpomeres 3 (p3, preapical) and 2 (p2) (p3/p2): **[0]** p2 not distinctly longer than p3 (maximum a3/a2 ratio 1.2); **[1]** p2 distinctly longer than p3.

(19) Maxillary palpus, relative length of palpomeres 4 (p4, apical) and 3 (p3, preapical) (p4/p3): **[0]** 1.5 at most; **[1]** longer than 1.5.

20 Maxillary palpus, relative width of palpomeres 4 (p4, apical) and 3 (p3, preapical) (p4/p3): **[0]** p4 not distinctly narrower than p3 for most of its length; **[1]** p4 distinctly narrower than p3 for most of its length.

(21) Maxillary palpus, palpomere 4 (apical), shape: **[0]** subacute, i.e., narrowed at base and evenly converging towards apex; **[1]** fusiform to expanded apically, i.e., narrowed at base but not (or not evenly) converging towards apex (Ramírez-Salamanca et al. 2020: fig. 3B); **[2]** subcylindrical "rod-like", parallel-sided at most of its length, apex subtruncate (Chani-Posse 2013: fig. 1A); **[3]** subcylindrical "rod-like", parallel-sided at most of its length, apex acute.

22 Prothorax, pronotum shape: **[0]** broadened posteriad; **[1]** parallel-sided or broadened at the anterior angles; **[2]** pronotum broadened anteriad behind the anterior angles.

23* Prothorax, pronotum, lateral margins: **[0]** straight and/or arcuate, not constricted before reaching posterior angles (Fig. 4A); **[1]** constricted before reaching posterior angles (Fig. 4B, C).

(24) Prothorax, pronotum, anterior angles: **[0]** not extended anteriad; **[1]** extended anteriad (Chani-Posse and Rodríguez-Melgarejo 2024: fig. 5A).

25 Prothorax, pronotum, posterior angles: **[0]** rounded to slightly obtuse (Ramírez-Salamanca et al. 2020: fig. 2A); **[1]** distinctly obtuse (Chani-Posse and Rodríguez-Melgarejo 2024: fig. 5A, B).

(26) Prothorax, pronotum, deflection, ventral view: **[0]** absent; **[1]** present.

27 Prothorax, large lateral setiferous puncture (llsp), position in relation to superior marginal line (sml) of pronotum (see Chani-Posse 2014a): **[0]** llsp situated very close to sml or at a distance no more than three times its diameter (fig. 4F); **[1]** llsp situated away from sml at a distance at least three times as large as its diameter (fig. 4G–I).

(28) Prothorax, hypomeron, inferior marginal line (iml), development (see Ramírez-Salamanca et al. 2020): **[0]** iml and sml gradually approaching each other for most of their length before meeting at anterior pronotal angle (apa) (fig. 4B); **[1]** iml and sml approaching each other shortly before meeting at apa (fig. 4A).

29 Prothorax, prosternum, shape of longitudinal carina: **[0]** forming well-defined, sharp ridge at least in its basal part; **[1]** more or less rounded, from obtuse ridge to smooth longitudinal prominence of prosternum.

30 Male protarsi, tarsomeres 2–3: **[0]** not bilobed (posterior margin moderately curved to straight); **[1]** sub-bilobed (Fig. 3C); **[2]** strongly bilobed (Chani-Posse 2014a: fig. 7F, G).

31 Male protarsi, tarsomeres 2–3, shape: **[0]** rectangular (i.e., flattened and rather transverse); **[1]** more or less cylindrical; **[2]** subtriangular (i.e., flattened and widened distally).

32 Protarsomeres 2–3, ventral surface, discal (adhesive) setae: **[0]** absent; **[1]** present.

33* Protarsomeres 2–3, ventral surface, discal setae (if present), distribution: **[0]** rather few, short and scattered (i.e., not forming a patch covering next segment) (Fig. 3E); **[1]** dense and distinctly long (i.e., forming a patch completely covering next segment) (Fig. 3F–H); **[2]** dense and moderately long (i.e., forming a patch not completely covering next segment) (Fig. 3K).

(34) Protarsomeres 2–3, ventral surface, discal setae (if present), shaft, microsculpture (see Chani-Posse and Ramírez-Salamanca 2020): **[0]** smooth (fig. 3C); **[1]** striate (fig. 3H).

(35) Protarsomeres 2–3, ventral surface, discal setae (if present), shaft, shape (see Chani-Posse and Ramírez-Salamanca 2020): **[0]** cylindrical, distinctly broadened apically (fig. 3B); **[1]** subcylindrical, gradually narrowed apically (fig. 3F).

36 Protarsomeres 2–3, ventral surface, marginal setae (see Chani-Posse and Ramírez-Salamanca 2020): **[0]** absent (if present only 1–2 fine setae at each lateroposterior angle) (fig. 2I, N, O); **[1]** present (e.g., fig. 2J, K, Q).

37 Protarsomeres 2–3, ventral surface, marginal setae, distribution (if present) (see Chani-Posse and Ramírez-Salamanca 2020): **[0]** posteriad (fig. 2Q); **[1]** lateral (fig. 2T).

38 Sexual dimorphism, profemur, shape: **[0]** absent (i.e., equally wide in both sexes); **[1]** present (i.e., wider in males).
39* Male profemora, shape: **[0]** not angulate medially; **[1]** distinctly angulate medially (Fig. 3D).
(40) Male profemora, spines, all along lateral face: **[0]** absent; **[1]** present.
41 Mesoventrite, intercoxal ridge (see Ramírez-Salamanca et al. 2020): **[0]** straight (fig. 3H); **[1]** arcuate (fig. 3G, I).
42* Mesotarsomere 2, ventral surface, discal setae: **[0]** absent and if so, barely visible; **[1]** present, distinct (Fig. 3I, J).
43* Elytral punctation: **[0]** slightly punctate (i.e., distance between punctures exceeding 2× diameter of puncture) (e.g., Figs 1A, D, 2A–F); **[1]** moderately to distinctly punctate (i.e., distance between punctures not exceeding 2× diameter of puncture).
(44) Elytra, surface shape: **[0]** distinctly flat; **[1]** with a couple of swellings.
45 Elytra, middle suture, elevation: **[0]** absent; **[1]** present.
(46) Abdomen, tergum 3, posterior basal transverse carina (PBTC): **[0]** absent; **[1]** present.
(47) Abdomen, tergum 4, PBTC: **[0]** absent; **[1]** present.
(48) Abdomen, tergum 5, PBTC: **[0]** absent; **[1]** present.
49 Abdomen, tergum 6, PBTC: **[0]** absent; **[1]** present.
50 Abdomen, sternum 3, basal transverse carina, shape: **[0]** arcuate; **[1]** acutely pointed to subangulate medially.
51 Abdomen, terga 3–7, setae: **[0]** almost glabrous; **[1]** scarcely setose (i.e., setae sparse and posteriad); **[2]** densely setose.
52 Abdomen, terga 3–5, rugose microsculpture, posterior basal transverse carina: **[0]** absent; **[1]** present.
53* Abdomen, tergum 8, hind margin: **[0]** not angulate medially (Fig. 5C, F); **[1]** angulate medially (Fig. 5Q).
(54) Male sternum 8, apical margin, notch (see Ramírez-Salamanca et al. 2020): **[0]** absent; **[1]** present (fig. 4E).
55 Male sternum 8, apical margin, emargination: **[0]** slight; **[1]** moderate; **[2]** deep.
(56) Male sternum 9, distal portion, emargination (if distinct): **[0]** acute; **[1]** subangulate to concave; **[2]** slightly arcuate.
57 Male sternum 9, basal portion, left end: **[0]** acute; **[1]** angulate; **[2]** rounded; **[3]** subacute.
58 Male tergum 10, shape: **[0]** emarginate medio-apically; **[1]** apically subtruncate to wide and subangulate or arcuate; **[2]** concave medio-apically to apically truncate; **[3]** apically distinctly subacute to acute.
59 Aedeagus, paramere(s), sensory peg setae: **[0]** absent; **[1]** present.
60 Aedeagus, paramere(s), degree of attachment to median lobe: **[0]** fused to median lobe only at base, otherwise paramere(s) distinctly separated from median lobe along entire length; **[1]** fused entirely to median lobe.
61 Aedeagus, paramere(s), shape: **[0]** elongate but rather flattened; **[1]** plate-like; **[2]** rod-like.
(62) Aedeagus, median lobe, apical half, lateral view (see Rodríguez-Melgarejo and Chani-Posse 2024): **[0]** bent downwards (fig. 1H); **[1]** not bent downwards (fig. 2H).
63 Aedeagus, median lobe, apical fourth, dorsal view: **[0]** gradually narrowed; **[1]** distinctly narrowed.
64 Aedeagus, median lobe, apex, dorsal view: **[0]** acute; **[1]** subacute to rounded.
65 Female tergum 10, shape: **[0]** emarginate medio-apically; **[1]** apically subtruncate to wide and subangulate or arcuate; **[2]** concave medio-apically to apically truncate; **[3]** apically distinctly subacute to acute.
66 Female abdomen, genitalia, accessory sclerite: **[0]** absent; **[1]** present.
67* Female abdomen, genitalia, accessory sclerite, shape (if present): **[0]** horseshoe-shaped (Fig. 5J, T); **[1]** linear (i.e., not curved, horseshoe or ring-shaped) (Ramírez-Salamanca et al. 2020: fig. 3J); **[2]** ring-shaped.

2.2.3. Procedure

Matrix analysis was performed using Mesquite v3.81 (Maddison and Maddison 2023), and three different inference approaches were applied: maximum parsimony (MP), maximum likelihood (ML), and Bayesian inference (BI). The MP analysis was conducted in TNT (Goloboff and Morales 2023), with 1,000 random addition sequence replicates followed by tree bisection-reconnection, and ten trees saved per replicate. Memory space was allocated for storing up to 99,999 trees. Clade support was evaluated by calculating absolute Bremer support values (BS) using the Bremer function in TNT, considering suboptimal trees up to 10 steps longer than the best tree. Character mapping was performed with WinClada v. 1.00.08 (Nixon 1999) employing unambiguous, fast, and slow optimization options. Synapomorphies, both exclusive and non-exclusive, were unambiguously optimized for the MP trees. For the most relevant nodes, only exclusive synapomorphies were reported for both fast and slow optimizations. For ML analysis, IQ-TREE v2.1.3 (Minh et al. 2020) was used, which allows for tree reconstruction (Nguyen et al. 2015) with an ultrafast bootstrap (UFB) approach (Hoang et al. 2018). The -bnni option was included to minimize the risk of overestimating branch support values due to model violations. Clade support in the ML analysis was evaluated with 1,000 bootstrap replicates for both the SH-aLRT and UFB tests (Guindon et al. 2010; Hoang et al. 2018).

Bayesian inference was conducted with MrBayes v. 3.2.7 (Ronquist et al. 2012), utilizing the Mkv model with default priors and a gamma distribution. Four chains were run for two independent runs of 10 million generations each, repeated twice. Convergence of the Markov Chain Monte Carlo (MCMC) was confirmed by evaluating the potential scale reduction factor (PSRF) and the average standard deviation of split frequencies (ASDF) using

Tracer v. 1.6 (Rambaut et al. 2014), based on the output from MrBayes.

In MP analysis, nodes with BS ≥ 2 were considered well-supported, while those with BS = 1 were regarded as weakly supported. For ML, nodes with SH-aLRT ≥ 80 and UFB ≥ 95 were considered well-supported, nodes with either SH-aLRT < 80 or UFB < 95 as weakly supported, and nodes with both SH-aLRT < 80 and UFB < 95 as unsupported. In BI analysis, nodes with Bayesian posterior probability (PP) ≥ 0.90 were deemed well-supported, PP values of 0.80–0.89 as weakly supported, and PP < 0.80 as unsupported. Nodes that were unsupported were typically not discussed when comparing topologies between methods or addressing monophyly.

All trees from both ML and BI analyses were visualized using FigTree v1.4.5_pre (Rambaut 2024).

3. Results

3.1. Taxonomy

Genus *Konradus* Chani-Posse & Ramírez-Salamanca, 2020

Figures 1A, B, 2A–C, 3E, 4A, 5A–J, 6A–C, 7, 8

Konradus Chani-Posse and Ramírez-Salamanca 2020: 239; Rodríguez-Melgarejo and Chani-Posse 2021: 16 (NT lineage); Chani-Posse et al. 2022: 65, 66, 70 (phylogeny); Ramírez-Salamanca et al. 2024: 5 (list); Chani-Posse et al. 2024: 118, 122 (phylogeny); Chani-Posse and Rodríguez-Melgarejo 2024: 396, 404, 405, 413 (phylogeny).

Species composition. Four species: *Konradus actinus* (Bernhauer) **comb. nov.** (Bolivia); *Konradus cuscensis* **sp. nov.** (Peru); *Konradus leehermani* Chani-Posse & Ramírez-Salamanca (Ecuador); *Konradus trescrucensis* **sp. nov.** (Peru).

Type species. *Konradus leehermani* Chani-Posse & Ramírez-Salamanca, 2020.

Diagnosis and description. As in Chani-Posse and Ramírez-Salamanca (2020a).

Recognition. *Konradus* can be easily recognized among other Neotropical genera of Philonthina by its distinct and entirely metallic-colored habitus, characterized by an elongate head and pronotum, with posterior angles of the head almost obsolete, gular sutures joined posteriorly before the neck, eyes distinctly shorter than the tempora, and protarsomeres 1–4 subequal in length, slightly to moderately widened apically, bearing both discal and marginal striate setae on the ventral surface, with the discal setae sparse and not forming a patch. Furthermore, *Konradus* can be distinguished from *Yuracarus* **gen. nov.** by several key features. The head of *Konradus* has posterior angles that are almost obsolete, while those of *Yuracarus* are distinctly obtuse. The profemur in *Konradus* is subcylindrical and not angulate medially, whereas in *Yuracarus* it is distinctly angulate in both sexes. Additionally, the protarsomeres 1–4 of *Konradus* have discal setae that are scattered and do not form a patch, in contrast to those of *Yuracarus*, where the discal setae form a patch on the ventral surface.

Distribution. *Konradus* is currently known from the Tropical Andes of Ecuador, with new records from Peru and Bolivia (Fig. 7), at altitudes ranging from 2100 to 3600 meters.

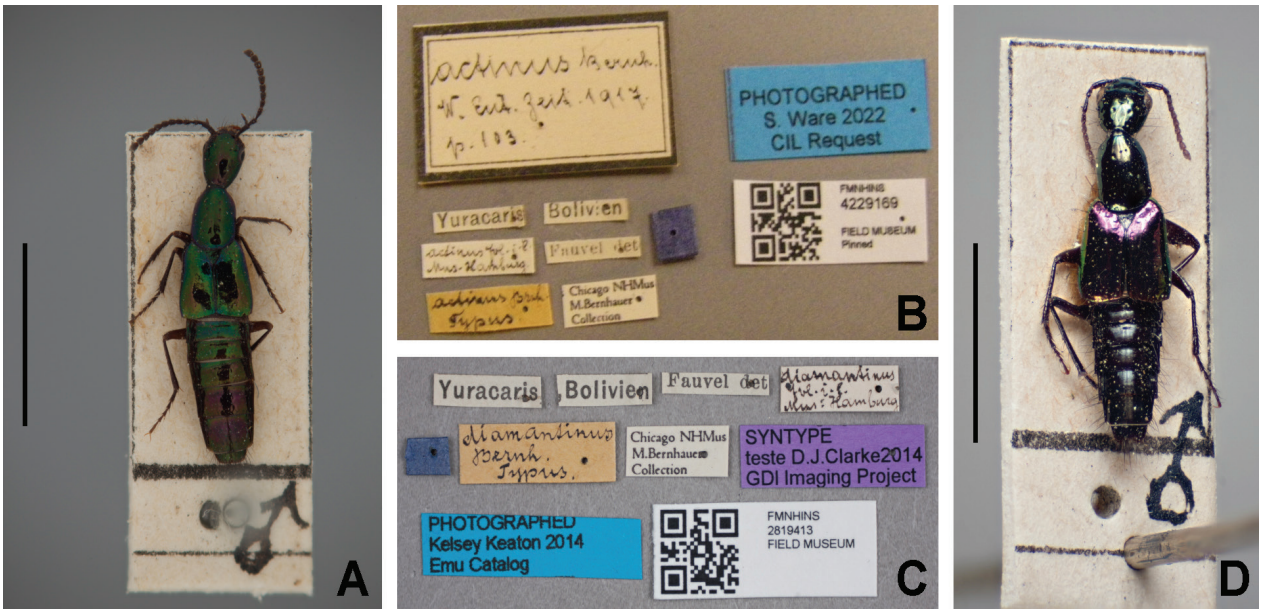

Figure 1. Type material. **A**, **B** *Philonthus actinus* Bernhauer and labels (HT, male) [FMNH ©]; **C**, **D** *Philonthus diamantinus* Bernhauer and labels (HT, male) [FMNH ©]. Scale bar: 4 mm.

Key to species of *Konradus* Chani-Posse & Ramírez-Salamanca, 2020

1 Head about as wide as pronotum (HW/PW = 1.0–1.1), pronotum parallel-sided, not narrowed posteriad (e.g. Fig. 1A) **2**
– Head wider than pronotum (HW/PW = 1.2), pronotum narrowed posteriad (Fig. 2A) ..... ***Konradus leehermani* Chani-Posse & Ramírez-Salamanca**
2 Antennomeres 7–8 elongate or quadrate, distance separating medial interocular punctures on frons at least 2.5× distance separating medial punctures from lateral punctures **3**
– Antennomeres 7–8 transverse, distance separating medial interocular punctures on frons not more than 2× distance separating medial punctures from lateral punctures ..... ***Konradus trescrucensis* sp. nov.**
3 Antennomeres 7–8 elongate, distance separating medial interocular punctures on frons 2.5× distance separating medial punctures from lateral punctures ..... ***Konradus actinus* (Bernhauer), new comb.**
– Antennomeres 7–8 quadrate, distance separating medial interocular punctures on frons 3× distance separating medial punctures from lateral punctures ..... ***Konradus cuscensis* sp. nov.**

Konradus leehermani Chani-Posse & Ramírez-Salamanca, 2020

Figures 2A, 3E, 4A, 7, 8

Konradus leehermani Chani-Posse & Ramírez-Salamanca, 2020: 241–243 (description, figures, distribution, phylogeny); Chani-Posse et al. 2022: 66 (phylogeny); Chani-Posse et al. 2024: 118, 122 (phylogeny); Chani-Posse and Rodríguez-Melgarejo 2024: 396, 404, 405 (phylogeny).

Diagnosis. *Konradus leehermani* can be identified among other species of *Konradus* by the following combination of characters: antennomeres 7–8 elongate, the distance separating the medial interocular punctures on the frons not more than twice the distance separating the medial punctures from the lateral punctures, the head wider than the pronotum at its widest point, and the pronotum narrowed posteriad.

Description and distribution. As in Chani-Posse and Ramírez-Salamanca (2020).

Konradus actinus (Bernhauer, 1917), comb. nov.

Figures 1A, B, 5A–D, 6A, 7, 8

Philonthus actinus Bernhauer 1917: 103, attributed to Fauvel in litteris; Scheerpeltz 1933: 1330 (catalog); Blackwelder 1944: 132 (list); Herman 2001: 2737 (catalog); Chani-Posse et al. 2018: 59 (checklist, "not *Philonthus*").

Type material. Lectotype ♂, here designated (Fig. 1A, B), with labels: [old white label with Bernhauer's handwriting] "actinus Bernh. / W. Ent. Zeit. 1917 / p. 103", [old white label printed] "Yuracaris", [old white label printed] "Bolivien", [old white label with Bernhauer's handwriting] "actinus fvl. i. l. / Mus. Hamburg", [old white label printed] "Fauvel det.", [yellow label with Bernhauer's handwriting] "actinus Brnh. / Typus" [white label printed] "Chicago NHMus / M. Bernhauer / Collection", [white label printed "FMNHINS / 4229169 / FIELD MUSEUM / Pinned", [blue label printed] "PHOTOGRAPHED / S. Ware 2022 / CIL Request", [red label] "Lectotype *Philonthus* / *actinus* Bernhauer 1917 / des. Chani-Posse et al. 2025" (FMNH). One paralectotype ♀ with same data, but yellow label with Bernhauer's handwriting with "actinus Brnh. / Cotypus" (FMNH).

Additional material examined. (2♂, 2♀). **BOLIVIA**: Cochabamba, 70 km NE Cochabamba, 4.IV.1978, L.& C.W. O' Brien & G.B. Marshall, 1♂ (FMNH); La Paz, Sorata, XI.1984, L.E. Peña, 2800m, 1♂, 2♀ (FMNH).

Diagnosis. *Konradus actinus* can be identified among other species of *Konradus* by the following combination of characters: antennomeres 7–8 elongate, the distance separating the medial interocular punctures on the frons 2.5× distance separating the medial punctures from the lateral punctures, the head as wide as pronotum at its widest point, and the pronotum parallel-sided.

Redescription. Body length 9.4–9.8 mm (5.4–5.6 mm, abdomen excluded), body overall scarcely setose, almost glabrous. — ***Colouration***: body metallic green, with last abdominal segments metallic purple to greenish purple. — ***Head***: moderately to slightly longer than wide (HW/HL= 0.8–0.9), as wide as pronotum at widest point (HW/PW= 1.0); epicranium with medial interocular punctures separated by distance 2.5× as large as distance separating medial punctures from lateral punctures. Eyes distinctly shorter than temples (EL/TL = 0.5–0.7) seen from above. Antennae with first antennomere distinctly shorter than second and third combined, third about 1.2–1.4× as long as second, fourth-eighth longer than wide, ninth-tenth about as long as wide. Labial palpus with third palpomere 1.5× as long as second. Maxillary palpus with fourth palpomere (apical) 1.6–1.8× as long as third. Neck about 0.4–0.5× as wide as head at widest point. — ***Pronotum***: distinctly to moderately longer than wide (PW/PL = 0.7–0.8), dorsal rows of punctures each with 5 punctures. Prosternum without distinct mid-longitudinal carina. — ***Legs***: Mesotarsi about as long as mesotibiae, metatarsi about as long as metatibiae, first metatarsomere shorter than fifth (S1/S5= 0.7–0.8). — ***Elytra***: at sides slightly longer than pronotum at midline (EtL/PL=1.1). — ***Male sexual characters***: Sternum 8 slightly emarginate medio-apically, emargination without semi-membranous

extension (Fig. 5A). Aedeagus with median lobe gradually narrowed from base to blunt, subacute apex, slightly constricted near paramere apex; internal sac with one pair of elongate, sclerotized structures (Fig. 6A). — ***Female sexual characters***: As described for genus (Fig. 5C, D), accessory sclerite horseshoe-shaped.

Geographical distribution. *Konradus actinus* is currently recorded only from the Tropical Andes of Bolivia, at elevations ranging from approximately 2000 m to 2800 m (Fig. 7).

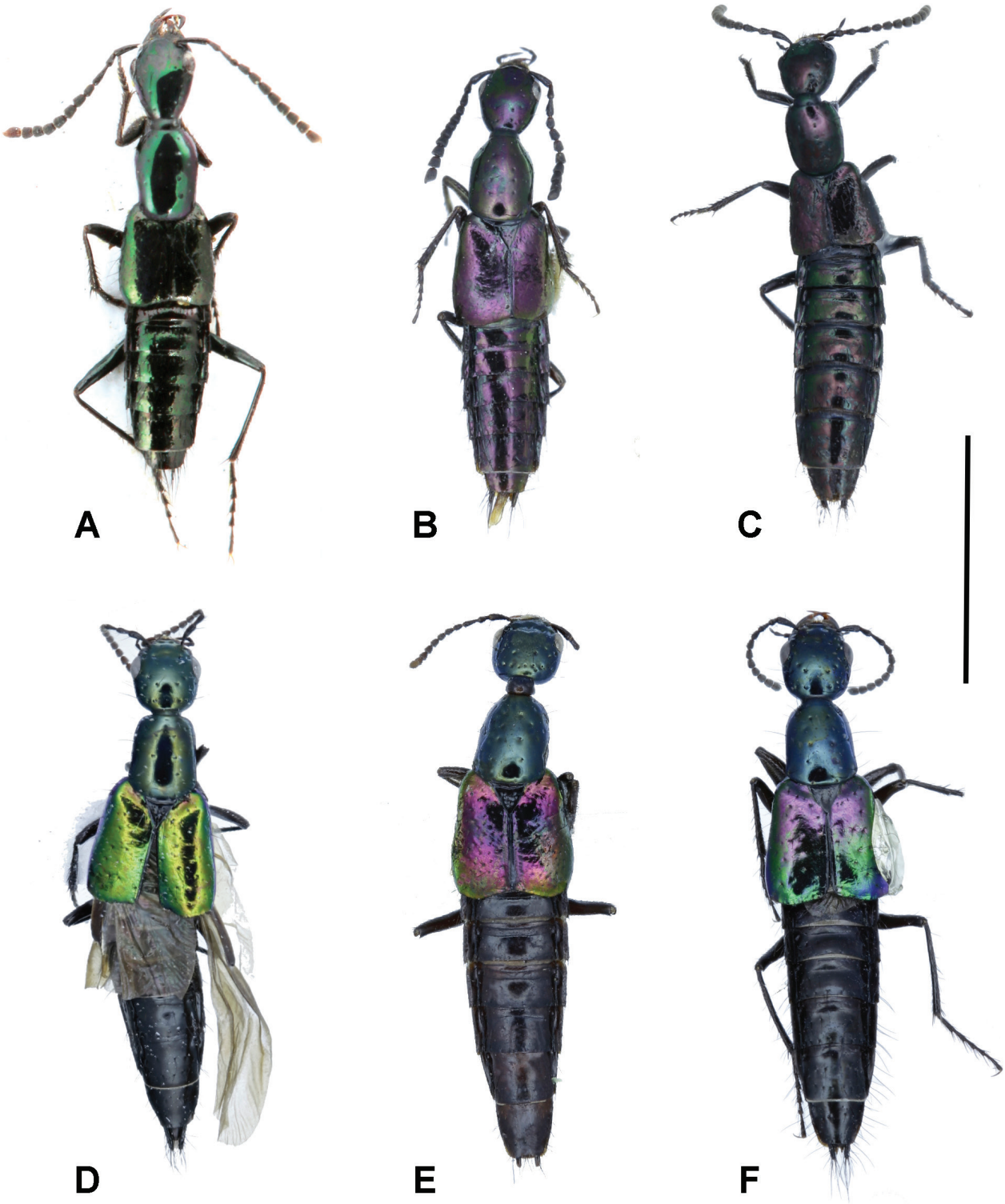

Figure 2. A *Konradus leehermani* Chani-Posse & Ramírez-Salamanca [NHMUK©]; **B** *Konradus cuscensis* **sp. nov.** (HT, male) [FMNH©]; **C** *Konradus trescrucensis* **sp. nov.** (PT, male) [MUSM©]; **D** *Yuracarus cosnipatensis* **sp. nov.** (PT, female) [MUSM©]; **E** *Yuracarus napoensis* **sp. nov.** (PT, female) [CNC©]; **F** *Yuracarus yunguensis* **sp. nov.** (PT, female) [FMNH©]. Scale bar: 5 mm.

Konradus cuscensis sp. nov.

https://zoobank.org/964EED6F-F19A-4C49-8A39-182483B70864

Figures 2B, 5F–J, 6B, 7, 8

Type material. Holotype ♂ (Fig. 2B), with labels: [white label] "PERU: Cuzco Dept., / Pillahuata, Manu rd. / km 126, 17-IX-1982", [white label] "FMHD #82-245, L. E. / Watrous & G. Mazurek", [red label] "Holotype *Konradus* / *cuscensis* Chani-Posse / et al. 2025" (FMNH). Two paratypes with same data, but 23-IX-1982, FMHD #82-280, 1♀ (FMNH) and 24-IX-1982, FMHD #82-284, 1♂ (FMNH). Both paratypes with additional red label: "Paratype *Konradus* / *cuscensis* Chani-Posse / et al. 2025".

Diagnosis. *Konradus cuscensis* can be identified among other species of *Konradus* by the following combination of characters: antennomeres 7–8 quadrate, the distance separating the medial interocular punctures on the frons at least 3.0× distance separating the medial punctures from the lateral punctures, the head as wide as pronotum at its widest point, and the pronotum parallel-sided.

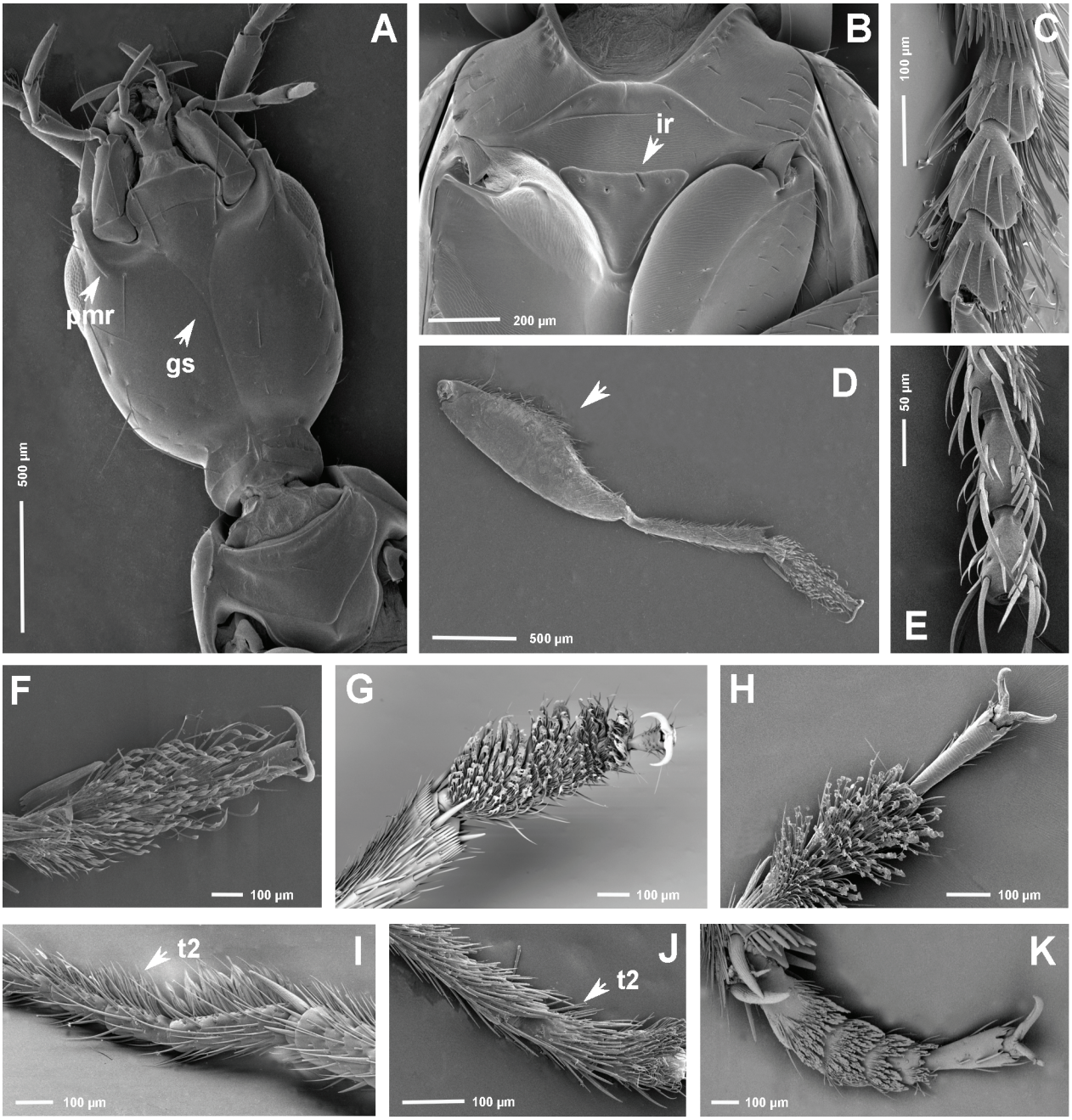

Figure 3. *Philonthus diamantinus* Bernhauer [CNC©]: **A** head in ventral view and prosternum; **B** mesosternum; **C** male protarsomeres 1–3 in dorsal view; **D** male proleg; **F** male protarsi in ventral view. *Konradus leehermani* Chani-Posse & Ramírez-Salamanca*:* **E** female protarsomeres 1–3 in ventral view. *Inesius callosipennis* (Bernhauer): **G** male protarsi in ventral view; **I** male mesotarsomeres 1–3 in dorsolateral view. *Delgadobius amazonensis* Chani-Posse & Couturier: **H** male protarsi in ventral view; **J** male mesotarsomeres 1–3 in dorsolateral view. *Philonthus splendens* (Fabricius): **K** male protarsi in ventral view. Abbreviations: pmr = postmandibular ridge, gs = gular sutures, ir = intercoxal ridge, t2 = mesotarsomere 2.

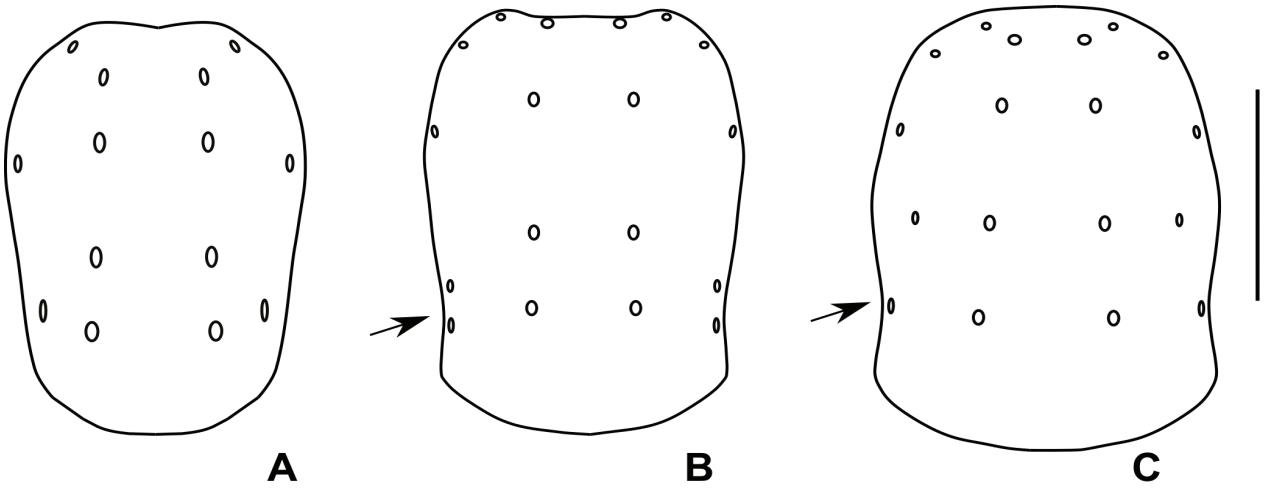

Figure 4. Pronotum: *Konradus leehermani* Chani-Posse & Ramírez-Salamanca (**A**), *Inesius callosipennis* (Bernhauer) (**B**), *Yuracarus diamantinus* (Bernhauer) (**C**). Scale bar: 1.0 mm.

Description. Body length 8.5–9.8 mm (5.2–5.9 mm, abdomen excluded), body overall scarcely setose, almost glabrous. — ***Colouration***: entire body varying from metallic purple to greenish purple. — ***Head***: distinctly longer than wide (HW/HL= 0.7), as wide as pronotum at widest point (HW/ PW= 1.0); epicranium with medial interocular punctures separated by distance 3× as large as distance separating medial punctures from lateral punctures. Eyes distinctly shorter than temples (EL/TL = 0.6) seen from above. Antennae with first antennomere distinctly shorter than second and third combined, third about 1.2× as long as second, fourth-sixth longer than wide, seventh-tenth about as long as wide. Labial palpus with third palpomere 1.5× as long as second. Maxillary palpus with fourth palpomere (apical) 1.7× as long as third. Neck about 0.6× as wide as head at widest point. — ***Pronotum***: distinctly longer than wide (PW/PL = 0.7), dorsal rows of punctures each with 5 punctures. Prosternum without distinct mid-longitudinal carina. — ***Legs***: Mesotarsi slightly shorter than mesotibiae, metatarsi about as long as metatibiae, first metatarsomere shorter than fifth (S1/S5= 0.9). — ***Elytra***: at sides as long as pronotum at midline (EtL/PL=1.0). — ***Male sexual characters***: Sternum 8 slightly emarginate medio-apically, emargination without semi-membranous extension. Aedeagus with median lobe distinctly narrowed apically into rather blunt, subacute apex, internal sac with one pair of elongate and sclerotized structures (Fig. 6B). — ***Female sexual characters***: As described for genus (Fig. 5I), accessory sclerite horseshoe-shaped (Fig. 5J).

Geographical distribution. *Konradus cuscensis* **sp. nov.** is currently recorded only from the locality of Pillahuata (Cosñipata district, Paucartambo province) from Cuzco department, in the Tropical Andes of Peru, at elevations beyond 2000 m (Fig. 7).

Etymology. The specific name *cuscensis* is a Latinized adjective referring to the locality of Cuzco, where this species was collected.

Konradus trescrucensis sp. nov.

https://zoobank.org/4125BC3E-058D-44AC-A761-B21B459A7415

Figures 2C, 5E, 6C, 7, 8

Type material. Holotype ♂, with labels: [white printed label] "PERU: CU, Tres Cruces / Abra Acjanaco, Bosque / Maderero, 3600m / ca. 13°18'S/ 71°40'W / 12.vii.1991 D. Silva", "Muestreo / por Golpeo", [red label] "Holotype *Konradus* / *trescrucensis* Chani-Posse / et al. 2025" (MUSM). One paratype with same data, ♂ (Fig. 2C), with additional red label: "Paratype *Konradus* / *trescrucensis* Chani-Posse / et al. 2025" (MUSM).

Diagnosis. *Konradus trescrucensis* can be identified among other species of *Konradus* by the following combination of characters: antennomeres 7–8 transverse, the distance separating the medial interocular punctures on the frons 2.0× distance separating the medial punctures from the lateral punctures, the head not distinctly wider than pronotum at its widest point, and the pronotum parallel-sided.

Description. Body length 8.5–8.8 mm (4.9–5.1 mm, abdomen excluded), body overall scarcely setose, almost glabrous. — ***Colouration***: head, thorax, elytra, and abdominal segments 6 and 7 metallic purple to purplish-green; scutellum and rest of abdomen metallic green. — ***Head***: slightly longer than wide (HW/HL= 0.9), as wide as to slightly wider than pronotum at widest point (HW/ PW= 1.0–1.1); epicranium with medial interocular punctures separated by distance 2.0× as large as distance separating medial punctures from lateral punctures. Eyes distinctly shorter than temples (EL/TL = 0.6) seen from above. Antennae with first antennomere moderately to slightly shorter than second and third combined, third about 1.2–1.4× as long as second, fourth and fifth longer than wide, sixth about as long as wide, seventh-tenth transverse. Labial palpus with third palpomere 1.5× as long as second. Maxillary palpus with fourth palpomere (apical) 2.0× as long

as third. Neck about 0.4× as wide as head at widest point. — ***Pronotum***: distinctly to moderately longer than wide (PW/PL = 0.7–0.8), dorsal rows of punctures each with 5 punctures. Prosternum without distinct mid-longitudinal carina. — ***Legs***: Mesotarsi slightly shorter than mesotibiae, metatarsi slightly shorter than metatibiae, first metatarsomere shorter than fifth (S1/S5= 0.8). — ***Elytra***: at sides as long as to slightly longer than pronotum at midline (EtL/PL=1.0–1.1). — ***Male sexual characters***: Sternum 8 slightly emarginate medio-apically, emargination without

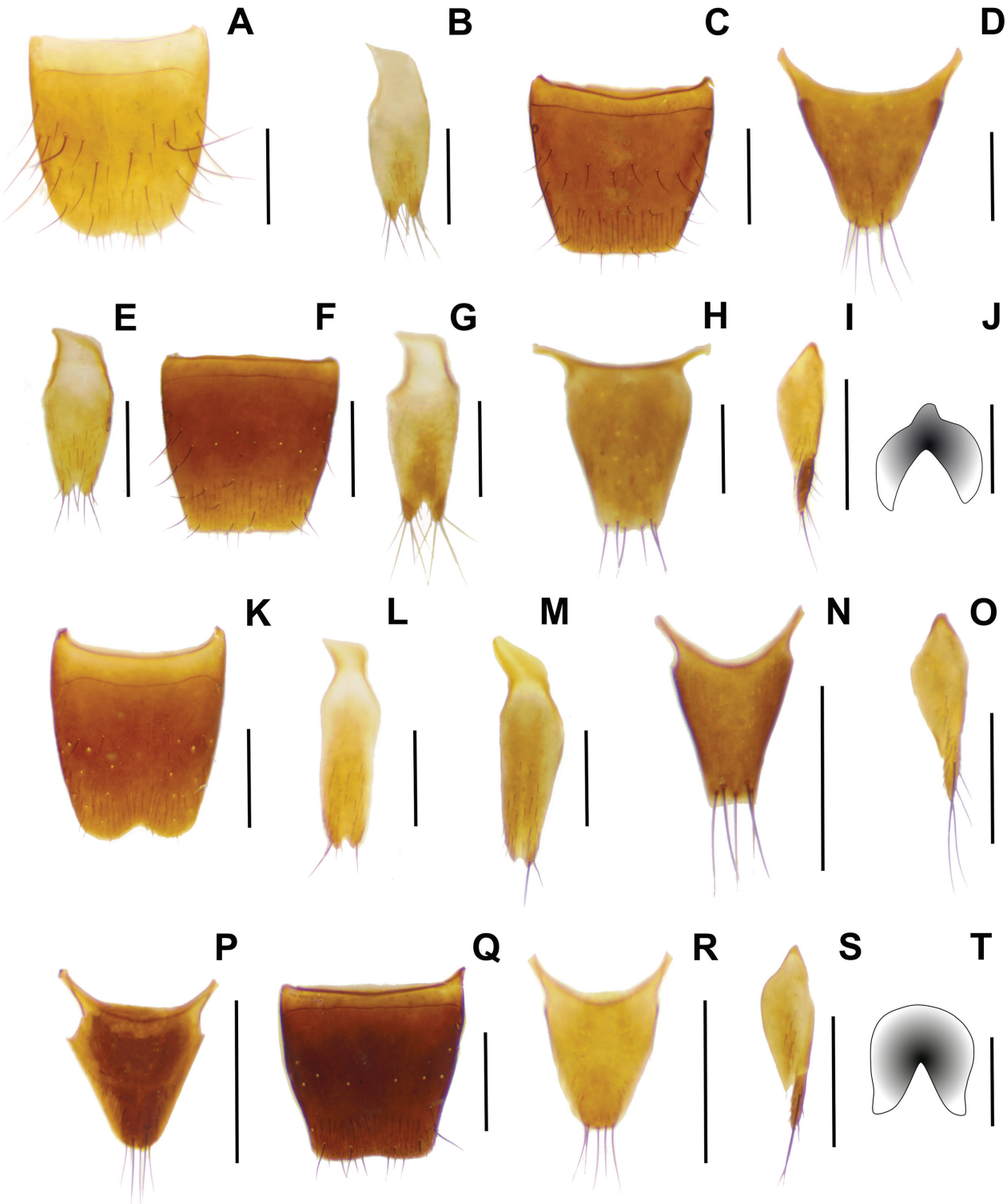

Figure 5. *Konradus actinus* (Bernhauer): **A** male sternum 8; **B** sternum 9; **C** female tergum 8; **D** female tergum 10. *Konradus trescrucensis* **sp. nov.**: **E** sternum 9. *Konradus cuscensis* **sp. nov**: **F** male tergum 8; **G** sternum 9; **H** male tergum 10; **I** gonocoxites of female genital segment; **J** accessory sclerite. *Yuracarus napoensis* **sp. nov.**: **K** male sternum 8; **L** sternum 9. *Yuracarus yunguensis* **sp. nov.**: **M** sternum 9; **N** male tergum 10; **O** gonocoxites of female genital segment; **P** female tergum 10. *Yuracarus cosnipatensis*: **Q** female tergum 8. *Yuracarus diamantinus* (Bernhauer): **R** female tergum 10; **S** gonocoxites of female genital segment; **T** accessory sclerite. Scale bars: 0.5 mm (A–I, K–S); 0.2 mm (J, T).

semi-membranous extension. Aedeagus with median lobe gradually narrowed from base into a subacute apex, internal sac with one pair of elongate and sclerotized structures (Fig. 6C). — ***Female sexual characters***: Unknown.

Geographical distribution. *Konradus trescrucensis* **sp. nov.** is currently recorded only from the locality of Tres Cruces (Cosñipata district, Paucartambo province) from Cuzco department, in the Tropical Andes of Peru, at 3600 m of altitude (Fig. 7).

Etymology. The specific name *trescrucensis* is a Latinized adjective referring to the locality of Tres Cruces, where this species was collected.

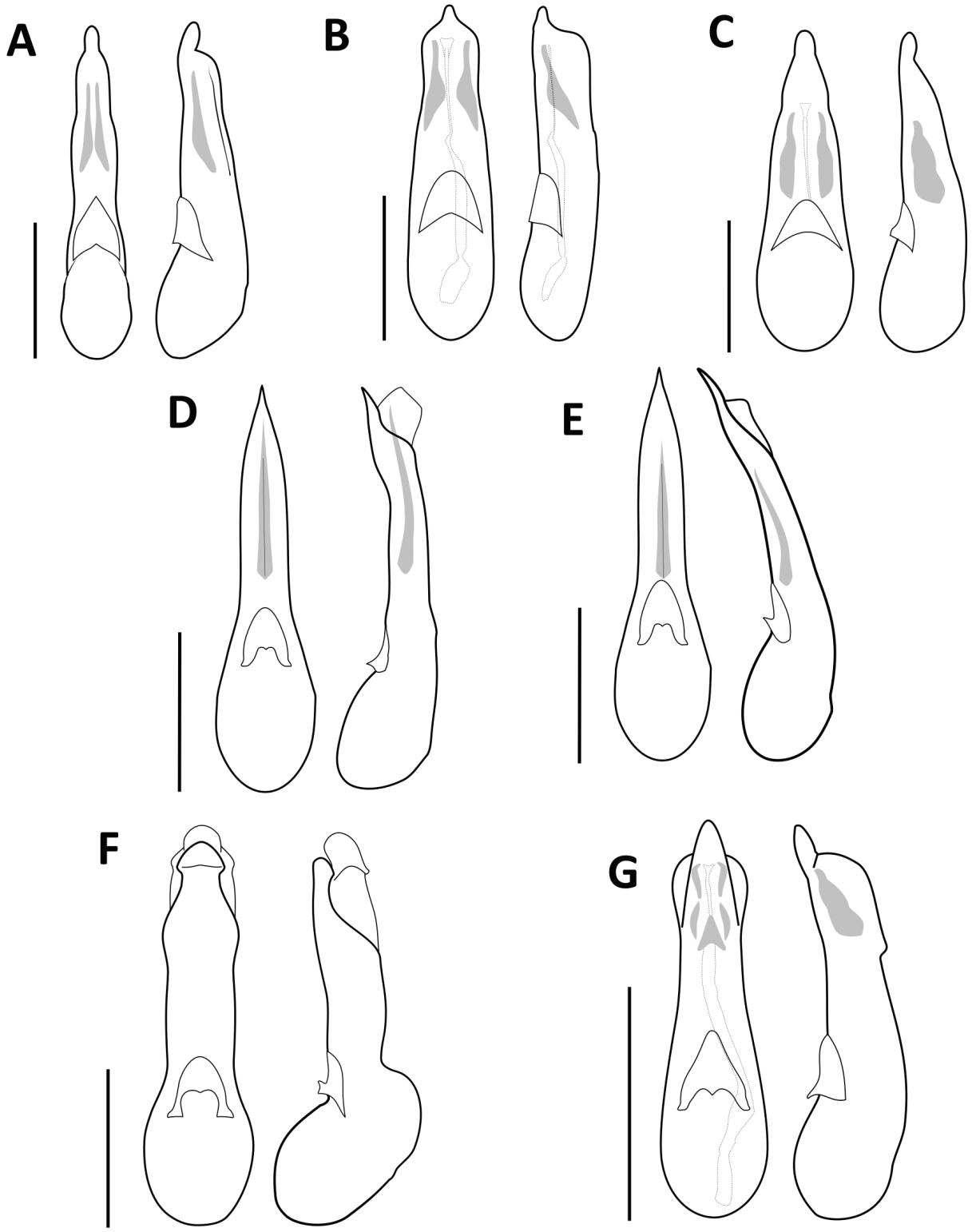

Figure 6. Aedeagus, dorsal and lateral views: **A** *Konradus actinus* (Bernhauer), **B** *Konradus cuscensis* **sp. nov.**, **C** *Konradus trescrucensis* **sp. nov.**, **D** *Yuracarus diamantinus* (Bernhauer), **E** *Yuracarus yunguensis* **sp. nov.**, **F** *Yuracarus cosnipatensis* **sp. nov.**, **G** *Yuracarus napoensis* **sp. nov.** Scale bars: 0.5 mm.

Genus *Yuracarus* gen. n.

https://zoobank.org/C3AB75DE-F553-4D4A-9CFD-71282EC69647

Figures 1C, D, 2D–F, 3A–D, F, 4C, 5K–T, 6D–G, 7–9

Species composition (four species): *Yuracarus cosnipatensis* **sp. nov.** (Peru); *Yuracarus diamantinus* (Bernhauer) **comb. nov.** (Bolivia); *Yuracarus napoensis* **sp. nov.** (Ecuador); *Yuracarus yunguensis* **sp. nov.** (Bolivia, Peru)

Type species. *Philonthus diamantinus* Bernhauer, 1917, here designated.

Diagnosis. The most distinctive characters of *Yuracarus* are its slender body shape, as well as its predominantly metallic-colored habitus (excluding the abdomen), in addition to the profemur distinctly angulate medially, the protarsomeres 1–4 enlarged, sub-bilobed, and rather flattened, with a patch of striate and petiolate discal setae, also present on the meso- and metatarsomeres, although less distinct due to the meso- and metatarsomeres being distinctly narrower than the protarsomeres, as well as the hind margin of tergum 8 truncate and angulate medially in both sexes. In addition to these characters, it differs from other Neotropical genera with enlarged protarsomeres and discal setae currently known (i.e., *Delgadobius*, *Konradus*, *Inesius*, *Rhaegalius* and *Atopocentrum*) by the gular sutures being joined anteriorly, whereas in *Delgadobius*, *Konradus*, *Inesius*, and *Rhaegalius*, the gular sutures are either joined posteriorly (*Konradus*, *Inesius*, *Rhaegalius* and *Atopocentrum*) or not joined (*Delgadobius*).

Description. Length 8.8–10.7 mm. Body elongate, more or less parallel sided, slightly widening toward elytra and tapering toward sixth visible abdominal segment, scarcely punctate (Fig. 1D). — ***Colouration***: Head, thorax and elytra of metallic colour, abdomen shiny black to piceous-black; antennae, palpi and legs piceous to piceous-black. — ***Head***: subrectangular shape with distinct hind angles (Figs 1D, 2D–F); about as long as to moderately longer than wide, as wide as to slightly narrower than pronotum at widest point; infraorbital ridge present, slightly extending beyond postgenal ridge; postgenal and ventral basal ridges present, well developed; postmandibular ridge present (Fig. 3A); epicranium with two pairs of interocular punctures, one medial puncture between interocular punctures; tempora with three to four postocular punctures arranged in line at each side; dorsal and ventral surface of head with distinctly sparse, fine punctuation and dense, wave-like microsculpture. Gular sutures joined anteriorly before neck (Fig. 3A). Eyes distinctly convex, moderately to distinctly shorter than temples seen from above. Antennae inserted closer to anterior margin of frontoclypeus than to eyes, separated from each other by at least 3.0× distance to eye, first antennomere less than one third of head length and distinctly shorter than antennomeres second and third combined, antennomere third slightly to distinctly longer than second, first three segments with rather scarce long setae, pubescence starting on segment fourth. Maxillary palpus with fourth palpomere longer than third (Fig. 3A). Labrum subtriangular, distinctly emarginate and completely sclerotized with numerous and long macrosetae at apical margin. Mentum with anterior margin slightly emarginate and about as long as submentum (Fig. 3A). Labial palpus moderately long, second palpomere about twice as long as first, third fusiform and distinctly longer than second (Fig. 3A). — ***Thorax***: Pronotum subcylindrical, slightly to distinctly longer than wide, parallel-sided, slightly constricted before reaching posterior angles (Fig. 4C); front margin subtruncate, hind margin arcuate, anterior obtusely rounded, posterior angles obtuse; lateral puncture of pronotum bearing long macroseta separated from superior line of pronotal hypomeron by distance no more than 3.0× as large as diameter of puncture; disc with dorsal rows of punctures sub-parallel to each other. Prosternum glabrous, without distinct mid-longitudinal carina; basisternum longer than furcasternum, with a rudimentary transverse carina (Fig. 3A). Mesoventrite somewhat elongate, with sternopleural suture distinctly oblique; mesoventral intercoxal process narrowly pointed forming sharp (subacute) angle and intercoxal ridge straight (Fig. 3B). — ***Legs***: Profemora enlarged and rather flattened, angulate medially, with scarce setae (Fig. 3D); protibiae setose, with 1–2 medio-apical spines; protarsi with first four segments subequal in length, moderately (female) to distinctly (male) widened and sub-bilobed apically, flattened dorsoventrally, ventral surface with both discal and marginal striate setae, discal setae striate and petiolate, forming a patch (Fig. 3C, D, F); meso- and metatibiae distinctly spinose; meso- and metatarsomeres narrower than protarsomeres, discal setae present. — ***Elytra***: at sides longer than pronotum at midline; punctuation fine and sparse (Figs 1D, 2D–F). — ***Abdomen***: Terga 3–6 with both anterior and posterior basal transverse carinae complete and straight (Figs 2E, F). Hind margin of tergum 8 truncate and angulate medially in both sexes. — ***Male sexual characters***: Sternum 8 emarginate medio-apically (Fig. 5K). Genital segment with lateral tergal sclerites 9 (styli) elongate and subcylindrical; tergum 10 truncate at apex with 3–4 apical setae and two subapical setae (Fig. 5N); sternum 9 with basal portion asymmetrical, distinctly shorter than distal portion and emarginate apically, distinctly setose at each side of emargination (Fig. 5L, M). Aedeagus with parameres fused as one short sclerite, completely fused to median lobe and without sensory peg setae; median lobe elongate, with apical part variably shaped (Fig. 6D–G). — ***Female sexual characters***: Sternum 8 with hind margin straight; tergum 10 truncate to arcuate at apex with 4–6 apical setae (Fig. 5P, R); second gonocoxites each with a long macroseta basally, with minute stylus (Fig. 5O, S) bearing one long macroseta and one distinctly short and fine seta. Accessory sclerite absent, or if present, horseshoe-shaped. — ***Immature stages***: Unknown.

Distribution. *Yuracarus* is currently known from the Tropical Andes of Ecuador, Peru and Bolivia (Fig. 7), at altitudes ranging from 2800 to 4100 meters.

Etymology. *Yuracarus* is a masculine, Latinized generic name derived from *Yuracaris*, the type locality of this new genus. The root "Yura-" is combined with the Latin suffix "-carus", denoting its association with the locality.

Key to species of *Yuracarus* gen. nov.

1 Antennomeres 8–10 quadrate, eyes at least 0.6× the length of temples **2**
– Antennomeres 8–10 elongate, eyes not longer than half the length of temples..... ***Yuracarus diamantinus*** (Bernhauer), **new comb.**
2 Distance separating medial interocular punctures on frons at least 2.5× distance separating medial punctures from lateral punctures **3**
– Distance separating medial interocular punctures on frons not more than 2.0× distance separating medial punctures from lateral punctures..... ***Yuracarus yunguensis*** **sp. nov.**
3 Head narrower than pronotum (HW/ PW = 0.9), distance separating medial interocular punctures on frons 3.0× distance separating medial punctures from lateral punctures ..... ***Yuracarus napoensis*** **sp. nov.**
– Head as wide as pronotum (HW/ PW = 1.0), distance separating medial interocular punctures on frons 2.5× distance separating medial punctures from lateral punctures..... ***Yuracarus cosnipatensis*** **sp. nov.**

Yuracarus cosnipatensis sp. nov.

https://zoobank.org/6D4CD43C-FBEF-44B2-A3A6-03695A821479

Figures 2D, 5Q, 6F, 7–9

Type material. Holotype ♂, with labels: [printed white label] "PERU: CU, Kosñipata, Wayqecha, / Wayqecha Trocha / Canopy 13°11'32.8"S, / 71°35'16.0"W, 2931 m", "02.xi.2017, cloud forest, / sifting of leaf litter, M. / Rodríguez & L. Pérez leg", [red label] "Holotype *Yuracarus* / *cosnipatensis* Chani-Posse / et al. 2025" (MUSM). Three paratypes: 1♀ with white handwritten label "PERU: CU, Cosñipata / Valley Centro / Investigación Wayqecha, / 2837 m, 13°11'20.9"S, / 71°35'4.08"W", 20.x.2007, / árboles caídos, C. Castillo" (MUSM), 1♀ with printed white label "PERU: CU, Kosñipata, / Wayqecha, trocha Canopy / I, 2986 m, 13°11'10.20"S, / 71°35'17.28"W, 27-30 / x.2019, trampas amarillas, / M. Rodríguez et al. leg" (MUSM) and 1♀ (Fig. 2D) with white printed label "PERU: CU, Cosñipata / Valley Centro / Investigación Wayquecha, / 2837 m, 13°11'20.9"S, / 71°35'4.8"W 20.x.2007, árboles caídos, C. Castillo" (MUSM). All paratypes with additional red label: "Paratype *Yuracarus* / *cosnipatensis* Chani-Posse / et al. 2025"

Diagnosis. *Yuracarus cosnipatensis* can be identified among other species of *Yuracarus* by the following combination of characters: antennomeres 8–10 quadrate, eyes at least 0.6× the length of the temples, the distance separating the medial interocular punctures on the frons at least 2.5× distance separating the medial punctures from the lateral punctures, and the head as wide as the pronotum (HW/PW = 1.0).

Description. Body length 8.8–9.0 mm (4.8–5.0 mm, abdomen excluded), body overall scarcely setose, almost glabrous. — ***Colouration***: Head and thorax dark metallic green, elytra goldish metallic green, abdomen shiny black to piceous-black; antennae, palpi and legs piceous to piceous-black. — ***Head***: about as long as wide (HW/ HL= 0.9–1.0), as wide as pronotum at widest point (HW/ PW= 1.0); epicranium with medial interocular punctures separated by distance 2.5× as large as distance separating medial punctures from lateral punctures. Eyes distinctly shorter than temples (EL/TL = 0.7) seen from above. Antennae with first antennomere moderately to distinctly shorter than second and third combined, third 1.2–1.3× as long as second, fourth-seventh longer than wide, eighth-tenth about as long as wide. Labial palpus with third palpomere 1.5× as long as second. Maxillary palpus with fourth palpomere (apical) 1.5× as long as third. Neck about 0.4–0.5x as wide as head at widest point. — ***Pronotum***: moderately to slightly longer than wide (PW/PL = 0.8–0.9), dorsal rows of punctures each with 4 punctures. **Legs**: Mesotarsi as long as mesotibiae, metatarsi slightly shorter than metatibiae, first metatarsomere shorter than fifth (S1/S5= 0.8). — ***Elytra***: at sides distinctly longer than pronotum at midline (EtL/PL=1.3). — ***Male sexual characters***: Sternum 8 deeply emarginate medio-apically. Aedeagus with median lobe distinctly narrowed at its apical fourth into a subacute apex, internal sac with one pair of elongate and sclerotized structures (Fig. 6F). — ***Female sexual characters***: As described for the genus, with tergum 10 arcuate apically.

Geographical distribution. *Yuracarus cosnipatensis* **sp. nov.** is currently recorded only from the locality of Cosñipata (Cosñipata district, Paucartambo province) in Cuzco department, from the Tropical Andes of Peru, at 2837 and 2931 m of altitude (Figs 7, 9).

Etymology. The specific name *cosnipatensis* is a Latinized adjective referring to the locality of Cosñipata, where this species was collected.

Yuracarus diamantinus (Bernhauer, 1917), comb. nov.

Figures 1C, D, 3A–D, F, 4C, 5R–T, 6D, 7, 8

Philonthus diamantinus Bernhauer 1917: 102, attributed to Fauvel in litteris; Scheerpeltz 1933: 1339 (catalog); Blackwelder 1944: 132 (list); Herman 2001: 2804 (catalog); Chani-Posse et al. 2018: 63 (checklist, "not *Philonthus*"); Chani-Posse and Ramírez-Salamanca 2020a: 199, 210, 211, 213 (phylogeny); Chani-Posse and Ramírez-Salamanca 2020b: 237–251 (characters, phylogeny); Ramírez-Salamanca et al. 2020: 151–167 (characters, phylogeny, figures).

Type material. Lectotype ♂, here designated (Figs 1C, D), with labels: [old white label printed] "Yuracaris", [old white label printed] "Bolivien", [old white label printed] "Fauvel det", [old white label with Bernhauer's handwriting] "diamantinus / fvl. i. l. / Mus. Hamburg", [yellow label with Bernhauer's handwriting] "diamantinus / Brnh. / Typus", [white label printed] "Chicago NHMus / M. Bernhauer / Collection", [purple label printed] "SYNTYPE / teste D. J. Clarke2014 / GDI Imaging Project", [white label printed] "FMNHINS / 2819413 / FIELD MUSEUM", [blue label printed] "PHOTOGRAPHED / Kelsey Keaton 2014 / Emu Catalog", [red label] "Lectotype *Philonthus* / *diamantinus* Bernhauer 1917 / des. Chani-Posse et al. 2025" (FMNH). One paralectotype ♀ with same data, but yellow label with Bernhauer's handwriting with "diamantinus Brnh. / Cotypus" (FMNH).

Additional material examined. BOLIVIA: Chapare, Yungas, 29–31.I.76, Bolle, 2900m, ♂ (CNC).

Diagnosis. *Yuracarus diamantinus* can be identified among other species of *Yuracarus* by the following combination of characters: antennomeres 8–10 elongate, eyes not longer than half the length of the temples, and the distance separating the medial interocular punctures on the frons not more than 2.0× distance separating the medial punctures from the lateral punctures.

Redescription. Body length 10.2–10.3 mm (5.0–5.2 mm, abdomen excluded), body overall scarcely setose, almost glabrous (Fig. 1D). — ***Colouration***: Head and thorax metallic green, elytra metallic purple to greenish purple, abdomen shiny black to piceous-black; antennae, palpi and legs piceous to piceous-black. — ***Head***: moderately to slightly longer than wide (HW/HL= 0.8–0.9), as wide as pronotum at widest point (HW/ PW= 1.0); epicranium with medial interocular punctures separated by distance 2.5× as large as distance separating medial punctures from lateral punctures. Eyes half shorter than temples (EL/TL = 0.5) seen from above. Antennae with first antennomere distinctly shorter than second and third combined, third about 1.3–1.4× as long as second, fourth-tenth longer than wide. Labial palpus with third palpomere 1.5× as long as second (Fig. 3 A). Maxillary palpus with fourth palpomere (apical) 1.3–1.4× as long as third (Fig. 3 A). Neck about 0.4× as wide as head at widest point. — ***Pronotum***: distinctly to moderately longer than wide (PW/PL = 0.7–0.8), dorsal rows of punctures each with 4 punctures. — ***Legs***: Mesotarsi shorter than mesotibiae, metatarsi shorter than metatibiae, first metatarsomere shorter than fifth (S1/S5= 0.8–0.9). — ***Elytra***: at sides moderately to distinctly longer than pronotum at midline (EtL/PL=1.2–1.3). — ***Male sexual characters***: Sternum 8 deeply emarginate medio-apically. Aedeagus

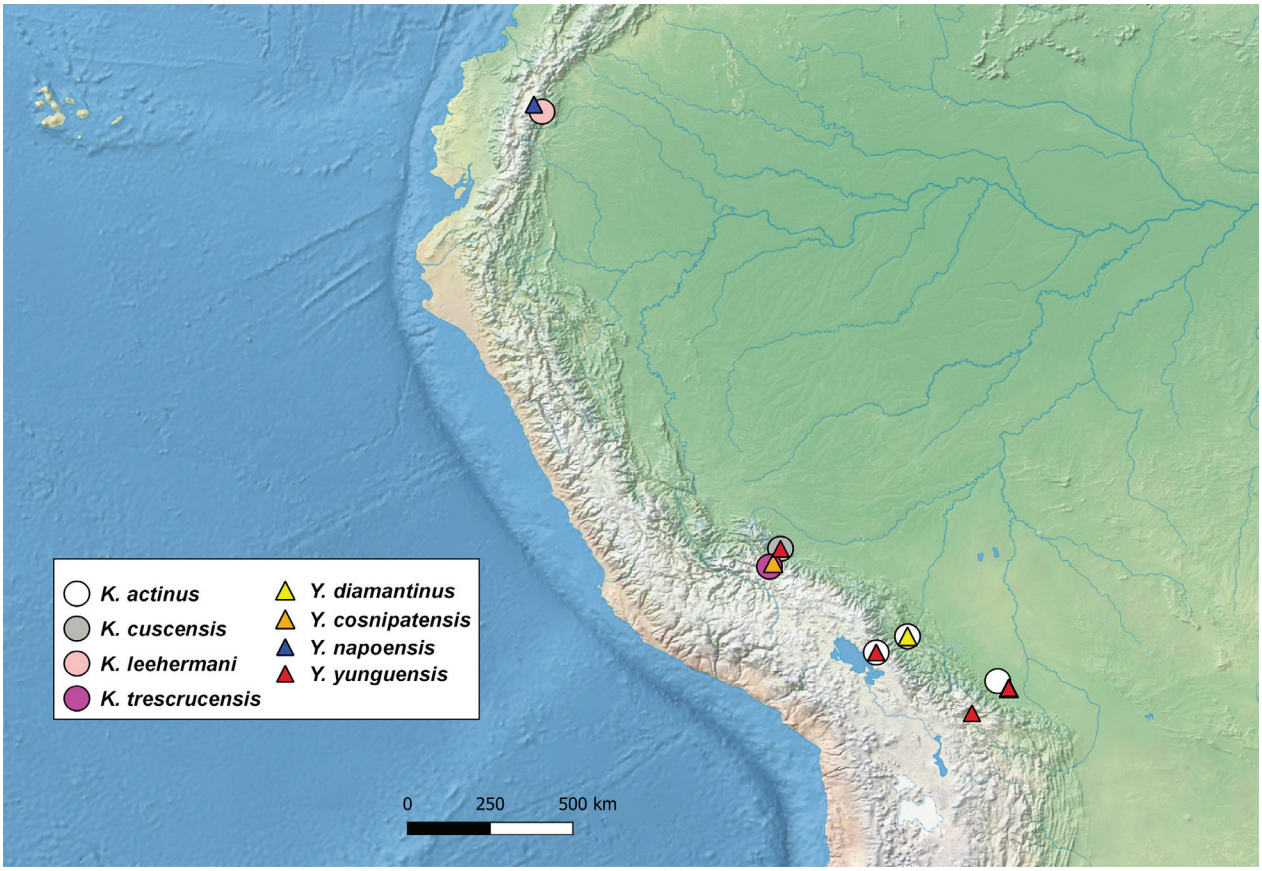

Figure 7. Distribution map for the species of *Konradus* Chani-Posse & Ramírez-Salamanca and *Yuracarus* **gen. nov.**

with median lobe gradually narrowed from base into rather acute apex, internal sac with one pair of elongate and sclerotized structures (Fig. 6D). — ***Female sexual characters***: As described for the genus, with tergum 10 truncate apically (Fig. 5R), accessory sclerite horseshoe-shaped (Fig. 5T).

Geographical distribution. *Yuracarus diamantinus* is currently recorded only from the Andes of Bolivia, at elevations ranging from approximately 2000 m to 2900 m (Fig. 7).

Yuracarus napoensis sp. nov.

https://zoobank.org/539D077B-C7E5-4D43-B72E-AB2F-DAADB2CA

Figures 2E, 5K, L, 6G, 7, 8

Type material. Holotype ♂, with labels: [white printed label] "ECU. Napo, 10200' / Papallacta / 21.V.82, H. Frania / canopy dead tree", [red label] "Holotype *Yuracarus* / *napoensis* Chani-Posse et al. 2025" (CNC). Seven paratypes: 2♂, 4♀ (Fig. 2E) with same data as above, one ♂ with white printed label "ECU. Napo, Baeza / 7800' 6.VI.1982 / H. Frania, ridge / top leaf litter" (CNC). All paratypes with additional red label: "Paratype *Yuracarus* / *napoensis* Chani-Posse / et al. 2025".

Diagnosis. *Yuracarus napoensis* can be identified among other species of *Yuracarus* by the following combination of characters: antennomeres 8–10 quadrate, eyes at least 0.6× the length of the temples, the distance separating the medial interocular punctures on the frons 3× distance separating the medial punctures from the lateral punctures, and the head narrower than pronotum (HW/PW = 0.9).

Description. Body length 9.6–10.7 mm (5.1–5.7 mm, abdomen excluded), body overall scarcely setose, almost glabrous. — ***Colouration***: Head and thorax metallic greenish blue, elytra mostly metallic purple to greenish purple apically, abdomen shiny black to piceous-black; antennae, palpi and legs piceous to piceous-black. — ***Head***: about as long as wide (HW/HL= 1.0), slightly narrower than pronotum at widest point (HW/ PW= 0.9); epicranium with medial interocular punctures separated by distance 3× as large as distance separating medial punctures from lateral punctures. Eyes distinctly shorter than temples (EL/TL = 0.6) seen from above. Antennae with first antennomere distinctly shorter than second and third combined, third 1.1× slightly longer than second, fourth-seventh longer than wide, eighth-tenth about as long as wide. Labial palpus with third palpomere 1.5× as long as second. Maxillary palpus with fourth palpomere (apical) 1.8× as long as third. Neck about 0.4× as wide as head at widest point. — ***Pronotum***: moderately longer than wide (PW/PL = 0.8), dorsal rows of punctures each with 4 punctures. — ***Legs***: Mesotarsi shorter than mesotibiae, metatarsi shorter than metatibiae, first metatarsomere shorter than fifth (S1/S5= 0.8). — ***Elytra***: at sides moderately longer than pronotum at midline (EtL/PL=1.2). — ***Male sexual characters***: Sternum 8 moderately emarginate medio-apically (Fig. 5K). Aedeagus with median lobe gradually narrowed from base into a subacute apex, internal sac with one pair of elongate and sclerotized structures (Fig. 6G). — ***Female sexual characters***: As described for the genus, with tergum 10 arcuate apically, accessory sclerite horseshoe-shaped.

Geographical distribution. *Yuracarus napoensis* **sp. nov.** is currently recorded only from the locality of Napo in the Andes of Ecuador, at approximately 2370 and 3100 m of altitude (Fig. 7).

Etymology. The specific name *napoensis* is a Latinized adjective referring to the locality of Napo, where this species was collected.

Yuracarus yunguensis sp. nov.

https://zoobank.org/750A2F4A-F96F-4A26-8119-101C6C86035A

Figures 2F, 5M–P, 6E, 7, 8

Type material. Holotype ♂, with labels: [white label] "BOLIVIA: La Paz: / Sorata, 2800m / XI.1984, L. E. Peña, leg. / FIELD MUS. NAT. HIST.", [red label] "Holotype *Yuracarus* / *yunguensis* Chani-Posse / et al. 2025" (FMNH). Seven paratypes: 1♂, 3♀ (Fig. 2F) with same data as above, 2♀ with white printed (except handwritten altitude and date) label "Bolivia: 4100m / Incachaca / Cochabambi / Coll. L. Pena / 31-VIII-1956 ", and 1♀ with two white printed labels "PERU: Cuzco Dept., / Pillahuata, Manu rd. / km 126, 24-IX-1982 "and "FMHD #82-264, on / tent, L. E. Watrous / & G. Mazurek" (FMNH). All paratypes with additional red label: "Paratype *Yuracarus* / *yunguensis* Chani-Posse / et al. 2025".

Diagnosis. *Yuracarus yunguensis* can be identified among other species of *Yuracarus* by the following combination of characters: antennomeres 8–10 quadrate, eyes at least 0.6× the length of the temples, and the distance separating the medial interocular punctures on the frons not more than 2.0× distance separating the medial punctures from the lateral punctures.

Description. Body length 9.2–10.7 mm (5.2–5.6 mm, abdomen excluded), body overall scarcely setose, almost glabrous. — ***Colouration***: Head and thorax metallic greenish blue, elytra mostly metallic purple basally to greenish blue apically, abdomen shiny black to piceous-black; antennae, palpi and legs piceous to piceous-black. — ***Head***: slightly longer than (HW/HL= 0.9), as long as pronotum at widest point (HW/ PW= 1.0); epicranium with medial interocular punctures separated by distance 2.0× as large as distance separating medial punctures from lateral punctures. Eyes moderately shorter than temples (EL/TL = 0.8) seen from above. Antennae with first antennomere distinctly shorter than second and third combined, third 1.1× slightly longer than second, fourth-seventh longer than wide, eighth-tenth about as

long as wide. Labial palpus with third palpomere 1.5× as long as second. Maxillary palpus with fourth palpomere (apical) 1.2× as long as third. Neck about 0.4× as wide as head at widest point. — ***Pronotum***: moderately longer than wide (PW/PL = 0.8), dorsal rows of punctures each with 4 punctures. — ***Legs***: Mesotarsi shorter than mesotibiae, metatarsi shorter than metatibiae, first metatarsomere slightly shorter than fifth (S1/S5= 0.9). — ***Elytra***: at sides distinctly longer than pronotum at midline (EtL/PL=1.3). — ***Male sexual characters***: Sternum 8 deeply emarginate medio-apically. Aedeagus with median lobe gradually narrowed from base into rather acute apex, internal sac with one pair of elongate and sclerotized structures (Fig. 6E). — ***Female sexual characters***: As described for the genus, with tergum 10 truncate apically (Fig. 5P).

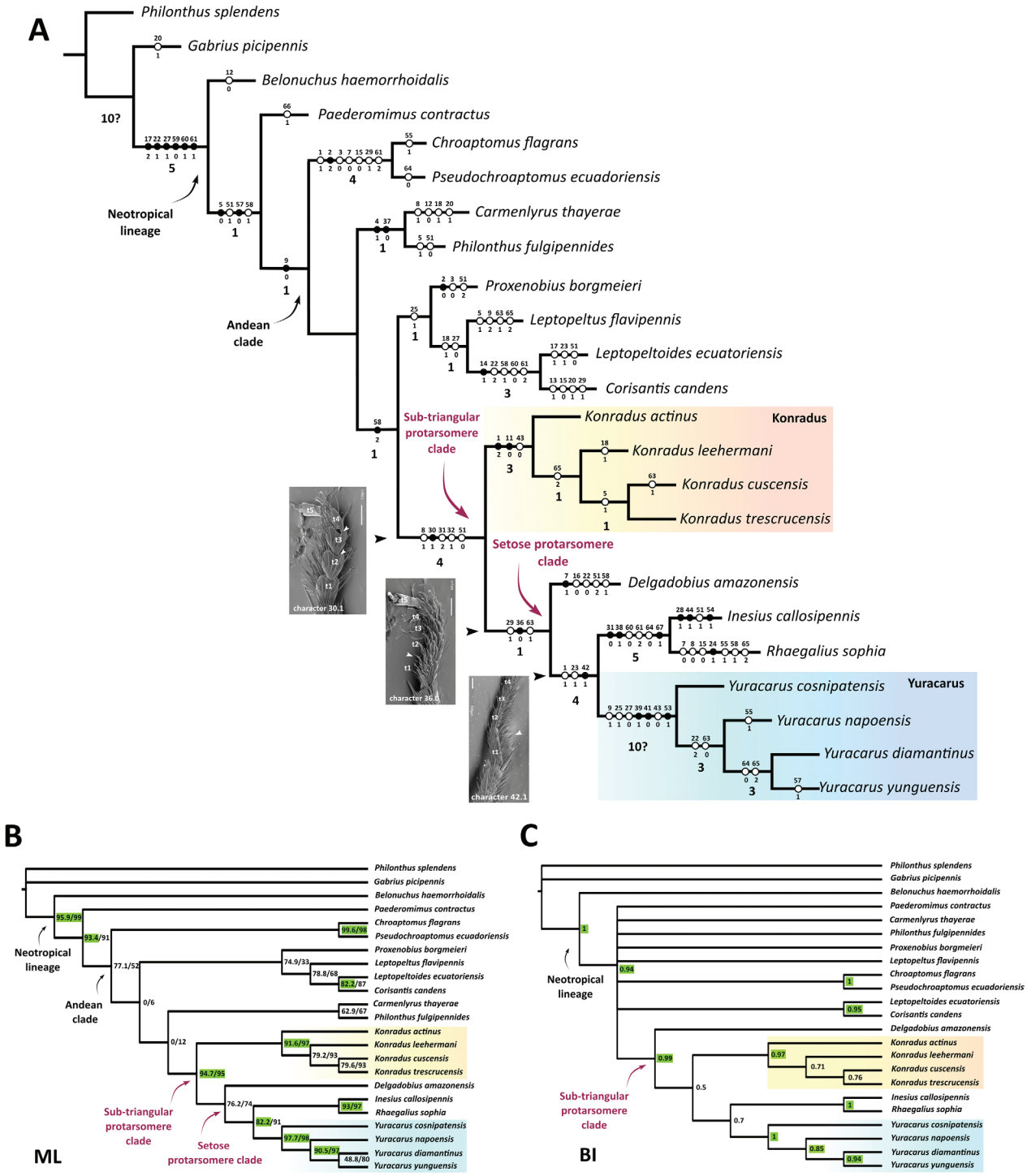

Figure 8. Phylogenetic reconstructions indicating relationships of *Konradus* Chani-Posse & Ramírez-Salamanca and *Yuracarus* **gen. nov.** within the Andean clade: **A** most parsimonious tree with black circles as exclusive (non-homoplastic) synapomorphies and white circles as non-exclusive (homoplastic) synapomorphies. Numbers in bold below the branches are absolute Bremer support values; **B** maximum Likelihood tree with support values SH-aLRT / UFB; **C** fifty percent majority consensus tree with posterior probabilities.

Geographical distribution. *Yuracarus yunguensis* **sp. nov.** is currently recorded from the Andes of Peru and Bolivia, at 2800 m and 4100 m of altitude (Fig. 7).

Etymology. The specific name *yunguensis* is a Latinized adjective referring to the Yungas ecoregion, where this species was collected.

3.2. Phylogeny

The analysis of the data matrix (File S1) produced one most parsimonious tree (MPT) (Fig. 8A) with 139 steps, a consistency index (CI) of 0.480, and a retention index (RI) of 0.700. The BI analysis converged well before 10 million generations, with the final average standard deviation of split frequencies (ASDSF) stabilizing at 0.0029. Average potential scale reduction factor (APSRF) values were 1.000, with a maximum value of 1.002.

Of the 21 nodes recovered by MP, 20 were supported by one, two, or all three inference methods. MP supported 20 nodes, while ML and BI each supported 10 nodes, respectively. The single MPT, along with the trees obtained by BI and ML and their support values, are shown in Fig. 8.

Overall, the consensus topologies recovered by MP, BI, and ML analyses were consistent at the generic level, showing that *Konradus* and *Yuracarus* each form distinct clades within a weakly supported AC only by MP (BS = 1). Incongruences mainly arose between MP and the model-based methods (ML and BI) in resolving basal relationships within the AC, with both ML and BI failing to resolve these relationships, unlike MP. Nonetheless, all three methods strongly support a group within the AC composed of *Delgadobius*, *Inesius*, *Rhaegalius*, *Konradus*, and *Yuracarus* (BS = 4, SH-aLRT = 94.7/UFB = 95, PP = 0.99). The monophyly of this group is also supported by one exclusive (30.1, male protarsomeres 2 and 3 sub-bilobed) and four non-exclusive (8.1*, head with protruding eyes; 31.2, male protarsomeres 2 and 3 subtriangular, i.e., flattened and widened distally; 32.1, male protarsomeres 2 and 3 with discal setae on ventral surface; 51.0, abdominal terga 3–7 almost glabrous) synapomorphies. Within this group,

Figure 9. Habitat of *Yuracarus cosnipatensis* **sp. nov.:** Peru, Cuzco, Cosñipata, Estación Biológica Wayqecha, 2837–2931 m. **A** Panoramic view of the cloud forest of the Cosñipata Valley; **B** Canopy trail; **C**, **D** Sifting of leaf litter along the Canopy trail.

both MP and ML resolve *Konradus* as the sister group to the remaining taxa which appear together in a clade only weakly supported by MP (BS =1) as well as one exclusive (36.0, protarsomeres 2–3 without marginal setae on ventral surface) and two non-exclusive (29.1, prosternum with longitudinal ridge more or less rounded, from obtuse ridge to smooth longitudinal prominence of prosternum; 63.1, median lobe of aedeagus with apical fourth gradually narrowed in dorsal view) synapomorphies. Within this clade, *Delgadobius* appears as the sister-group to a subclade composed of *Inesius*, *Rhaegalius* and *Yuracarus*, weakly supported by MP and ML (BS = 4, SH-aLRT = 82.2/UFB = 91) as well as one exclusive (42.1*, mesotarsomere 2 with discal setae on ventral surface) and two non-exclusive (1.1*, body with metallic coloration limited to head, thorax and elytra; 23.1*, pronotum with lateral margins constricted before reaching posterior angles) synapomorphies. Within this subclade, the relationship between *Inesius* + *Rhaegalius* is strongly supported as a monophyletic group by all methods (BS = 5, SH-aLRT = 93/UFB = 97, PP = 1) alongside three exclusive (31.0, male protarsomeres 2 and 3 rectangular, i.e., flattened and rather transverse; 38.1, profemur sexually dimorphic, i.e., wider in males; 67.1, female genitalia with accessory sclerite linear) and three non-exclusive (60.0, paramere fused to median lobe only at base and 61.2, plate-like; 64.0, aedeagus with median lobe acute apically in dorsal view) synapomorphies, with *Yuracarus* as the sister group. Both *Konradus* and *Yuracarus* appear as monophyletic groups, strongly supported by all three methods (*Konradus*: BS = 3, SH-aLRT = 91.6/UFB = 97, PP = 0.97; *Yuracarus*: BS = 10?, SH-aLRT = 97.7/UFB = 98, PP = 1). *Konradus* is also defined by two exclusive (1.2*, entire body with metallic coloration; 11.0*, head with posterior angles almost obsolete) and one non-exclusive (43.0, elytra slightly punctate). *Yuracarus* is defined by three exclusive (39.1*, male profemora distinctly angulate medially; 41.0, mesoventrite with intercoxal ridge straight; 53.1*, abdominal tergum 8 with hind margin angulate medially in both sexes) and four non-exclusive (9.1, maximum width of head at its halfway between the anterior and posterior margin; 25.1, pronotum with posterior angles distinctly obtuse; 27.0, pronotum with large lateral setiferous puncture situated very close to superior marginal line of pronotum or at a distance no more than three times its diameter; 43.0*, elytra slightly punctate) synapomorphies.

Internal relationships within *Konradus* are weakly supported only by MP, with *K. actinus* as the sister taxon to the remaining three species (BS = 1) within which *K. cuscensis* and *K. trescrucensis* are sister taxa. In contrast, internal relationships within *Yuracarus* are supported by all three methods, with exception of *K. diamantinus* + *K. yunguensis*, unsupported by ML. Within *Yuracarus*, *Y. cosnipatensis* appears as the sister group to the remaining three species (BS = 3, SH-aLRT = 90.5/UFB = 97, PP = 0.85).

For the most relevant nodes (see Fig. 8) fast optimization recovered six additional exclusive synapomorphies, while slow optimization found only one additional. These include: 67.0, female genitalia with accessory sclerite elongate or short, not ring-shaped or horseshoe-shaped, for the Andean clade (AC, fast optimization) and for the "sub-triangular protarsomere" clade composed of *Delgadobius*, *Inesius*, *Rhaegalius*, *Konradus*, and *Yuracarus* (slow optimization). Additionally, fast optimization also identified 16.2, gular sutures joined rather close to the base of the head, for the latter group, along with 33.1, protarsomeres 2 and 3 with dense, distinctly long discal setae on the ventral surface, and 55.2, male sternum 8 deeply emarginate apically, further defining the clade composed of *Delgadobius*, *Inesius*, *Rhaegalius*, and *Yuracarus*. Furthermore, the clade (*Inesius* + *Rhaegalius*) + *Yuracarus* is supported by synapomorphies 45.1, elytra with an elevated middle suture, and 51.1, abdominal terga 3–7 scarcely setose.

4. Discussion

The revision of type and non-type material collected from the Andes of Ecuador, Peru, and Bolivia, and deposited in entomological collections, led to an increase in the number of species in the previously monotypic and recently described genus *Konradus*, as well as the discovery of a new genus, *Yuracarus*. Additionally, two species originally described as *Philonthus* (*Ph. actinus* and *Ph. diamantinus*), but previously identified as "false" *Philonthus* species (e.g., Chani-Posse and Ramírez-Salamanca 2020b), were reclassified into the aforementioned genera. The monophyly of both *Konradus* and *Yuracarus* was supported in all morphological-based reconstructions performed herein, with both genera placed in a well-supported group alongside *Inesius*, *Rhaegalius*, and *Delgadobius* within the AC of Philonthina. A key character defining this group is the configuration of protarsomeres 2 and 3, which are subtriangular (i.e., flattened and widened apically), sub-bilobed apically, and bear discal setae on their ventral surface. Although this condition has traditionally been considered a plesiomorphic character in the broader context of Philonthina and other rove-beetles (e.g., Chani-Posse and Ramírez-Salamanca 2020b; Spiessberger et al. 2024), it becomes phylogenetically significant within its NL. In fact, the configuration of protarsomeres and the associated discal setae is unique within the NL and serves to distinguish them from all other members including Holarctic taxa (e.g., Chani-Posse 2014b; Chani-Posse and Ramírez-Salamanca 2020b).

Furthermore, within the subtriangular protarsomere clade, two additional traits emerge as particularly significant when unambiguously optimized. These include the presence of an accessory sclerite located along and between the gonocoxites and tergum 10, found in all genera of this group, including *Konradus*, and the dense, distinctly long discal setae of the protarsomeres 2 and 3, present in all genera except *Konradus*. While these traits, particularly the discal setae, may show dubious homology when observed outside this group, their uniqueness within the NL and the AC supports their inclusion as key synapomorphies. It should be noted that these derived

characters were also observed in species outside the AC, within Philonthina. For instance, the occurrence of discal setae (which are also long and dense in some species of *Cafius* Stephens, 1829) and the accessory sclerite (which appears in *Ph. splendens* and some species of *Paederomimus*). However, the non-homology of the discal setae between the Holarctic representatives of Philonthina (including *Cafius*) and members of the AC has been previously proposed (Chani-Posse and Ramírez-Salamanca 2020b). Furthermore, the shape of the accessory sclerite, which is horseshoe-shaped or linear within the AC, contrasts with the ring-like shape observed in *Philonthus splendens* and some species of *Paederomimus*. Accordingly, we propose that the group composed of taxa with sub-bilobed and subtriangular protarsomeres 2 and 3, bearing dense and distinctly long discal setae on their ventral surface (dense and long in all representatives except *Konradus*), as well as a horseshoe-shaped accessory sclerite associated with female tergum 10, constitutes a well-supported clade within the AC of the NL. This clade could serve as a reliable hypothesis for the systematic placement of unidentified Andean species of Philonthina exhibiting these characters in future studies.

A possible hypothesis to explain the presence of dense, distinctly long discal setae on the ventral surface of the protarsomeres in Philonthina species inhabiting coastal (e.g., *Cafius*) or cloud forest (e.g., *Yuracarus*, *Inesius*) environments is that these structures may serve as an adaptation to enhance grip and stability on slippery, dynamic substrates, such as wet rocks, dense vegetation, or seaweed. Long setae may help prevent displacement by precipitation or water currents and facilitate the sensory detection of prey movements in fluctuating environments. In contrast, species of *Philonthus* living in more stable habitats, such as compost or forest soils, exhibit shorter setae, which are sufficient for maintaining traction and detecting vibrations in less dynamic conditions. This contrast suggests that setae length may be functionally linked to the stability and moisture characteristics of the beetle's habitat. Thus, if a trait that might initially appear convergent (species of *Cafius* versus those of *Yuracarus* and allied genera) is present in the common ancestor of a group and accompanies the radiation of that group (i.e., *Delgadobius*, *Inesius*, *Rhaegalius*, and *Yuracarus*), it would no longer be regarded as convergence. Building on this, the dense, long discal setae present in the protarsomeres of *Cafius* and the aforementioned group are not homologous between these two groups, as they likely evolved independently in response to similar ecological pressures, particularly those associated with dynamic and slippery substrates such as coastal rocks, seaweeds, or the often wet canopy vegetation typical of cloud forests. However, within the "setose protarsomere" clade the presence of these setae would be homologous, as they are inherited from their common ancestor and provide consistent phylogenetic signal. This further supports the hypothesis that these characters define a distinct and well-supported clade within the AC of the NL.

In conclusion, the presence of these setae, along with other derived characters, can be used to recognize and define a specific clade within the AC, strengthening the case for their phylogenetic relevance and aiding in the systematic classification of these taxa. Future studies should continue to explore the evolutionary and ecological significance of these traits, further elucidating the mechanisms driving diversification within this fascinating group of beetles in the Neotropical region.

5. Funding

This study was financed by Consejo Nacional de Investigaciones Científicas y Técnicas (CONICET) [PIP DD87 (M. Chani-Posse and F. Agrain)] and Agencia Nacional de Promoción Científica y Tecnológica (ANPCyT) – Fondo para la Investigación Científica y Tecnológica (FONCYT) [PICT 2019-03121 (M. Chani-Posse and F. Agrain)].

6. Competing interests

The authors have declared that no competing interests exist.

7. Acknowledgements

We gratefully acknowledge the help received from all museum curators here when loaning the specimens. We also thank the Willi Hennig Society for the free use of TNT. MRM thanks to Conservación Amazónica – ACCA for the scholarship awarded to carry out field trips at the Estación Biológica Wayqecha (2017 and 2019) where *Yuracarus cosnipatensis* was collected.

8. References

Bernhauer M (1917) Neue sudamerikanische Staphyliniden (18. Beitrag). Wiener Entomologische Zeitung 36(3–5): 102–116. https://doi.org/10.5962/bhl.part.12925

Blackwelder RE (1944) Checklist of the coleopterous insects of Mexico, Central America, the West Indies, and South America. Part 1. Bulletin of the United States National Museum 185: 1–188. https://doi.org/10.5479/si.03629236.185.i

Chani-Posse M (2013) Towards a natural classification of the subtribe Philonthina (Coleoptera: Staphylinidae: Staphylinini): a phylogenetic analysis of the Neotropical genera. Systematic Entomology 38(2): 390–406. https://doi.org/10.1111/syen.12003

Chani-Posse M (2014a) An illustrated key to the New World genera of Philonthina Kirby (Coleoptera: Staphylinidae), with morphological, taxonomical and distributional notes. Zootaxa 3755(1): 62–86. https://doi.org/10.11646/zootaxa.3755.1.3

Chani-Posse M (2014b) Systematics and phylogeny of the Neotropical genera *Pescolinus* Sharp and *Neopescolinus* gen.n. (Coleoptera: Staphylinidae). Arthropod Systematics and Phylogeny 72(3): 237–255. https://doi.org/10.3897/asp.72.e31788

Chani-Posse MR, Brunke AJ, Chatzimanolis S, Schillhammer H, Solodovnikov A (2018a) Phylogeny of the hyper-diverse rove beetle subtribe Philonthina with implications for classification of the tribe Staphylinini (Coleoptera: Staphylinidae). Cladistics 34: 1–40. https://doi.org/10.1111/cla.12188

Chani-Posse M, Couturier G (2012) *Delgadobius amazonensis* – a new genus and species of the subtribe Philonthina from Amazonia

(Coleoptera: Staphylinidae: Staphylininae). Zootaxa 3568: 81–88. https: //doi.org/10.11646/zootaxa.3568.1.6

Chani-Posse M, Newton A, Hansen A, Solodovnikov A (2018b) Checklist and taxonomic changes for Central and South American Philonthina (Coleoptera: Staphylinidae). Zootaxa 4449(1): 1–95. https://doi.org/10.11646/zootaxa.4449.1.1

Chani-Posse MR, Ramírez-Salamanca JM (2020a) To be biased or to be Neotropical: systematic reassessment of a megadiverse lineage of rove-beetles (Philonthina, Staphylinini, Staphylininae). Cladistics 36: 194–217. https://doi.org/10.1111/cla.12395

Chani-Posse MR, Ramírez-Salamanca JM (2020b) *Konradus leehermani* – a new genus and species of Philonthina from the Neotropical region and its phylogenetic relationships (Coleoptera: Staphylinidae: Staphylininae). Zootaxa 4759(2): 237–251. https://doi.org/10.11646/zootaxa.4759.2.6

Chani-Posse MR, Ramírez-Salamanca JM, Silva-Tavera DF (2022) Systematic treatment of the Neotropical Philonthina (Coleoptera, Staphylinidae, Staphylinini): *Carmenlyrus* **gen. nov.** and its phylogenetic relationships. Zoologischer Anzeiger 299: 62–72. https://doi.org/10.1016/j.jcz.2022.04.004

Chani-Posse MR, Rodríguez-Melgarejo ME (2024) Origin and early diversification of a high Andean rove-beetle clade: *Corisantis* **gen. nov.**, phylogeny, and historical biogeography. Zoologischer Anzeiger 313: 395–416. https://doi.org/10.1016/j.jcz.2024.11.002

Guindon S, Dufayard JF, Lefort V, Anisimova M, Hordijk W, Gascuel O (2010) New algorithms and methods to estimate maximum-likelihood phylogenies: assessing the performance of PhyML 3.0. Systematic Biology 59(3): 307–321. https://doi.org/10.1093/sysbio/syq010

Goloboff PA, Morales ME (2023) TNT version 1.6, with a graphical interface for MacOS and Linux, including new routines in parallel. Cladistics 39: 144–153. https://doi.org/10.1111/cla.12524

Herman LH (2001) Catalog of the Staphylinidae (Insecta: Coleoptera). 1758 to the end of the second millennium. Part V. Bulletin of the American Museum of Natural History 265: 2441–3020. http://hdl.handle.net/2246/5826

Hoang DT, von Chernomor O, Haeseler A, Minh BQ, Vinh LS (2018) UFBoot2: Improving the ultrafast bootstrap approximation. Molecular Biology and Evolution 35: 518–522. https://doi.org/10.1093/molbev/msx281

Horn W, Kahle I, Friese G, Gaedike R (1990) Collectiones Entomologicae. Ein Kompendium über den Verbleib entomologischer Sammlungen der Welt bis 1960. Teil I: A bis K und Teil II: L bis Z. Akademie der Landwirtschaftswissenschaften der Deutschen Demokratischen Republik, Berlin, 220 pp. (Teil I), 353 pp. (Teil II).

Maddison WP, Maddison DR (2023) Mesquite: a modular system for evolutionary analysis. Version 3.81. Available at: http://www.mesquiteproject.org

Minh BQ, Schmidt HA, Chernomor O, Schrempf D, Woodhams MD, Von Haeseler A, Lanfear R, Teeling E (2020) IQ-TREE 2: New Models and Efficient Methods for Phylogenetic Inference in the Genomic Era. Molecular Bioloy and Evolution 37: 1530–1534. https://doi.org/10.1093/molbev/msaa015

Newton A (2025) StaphBase (version Aug 2022). In: Bánki O, Roskov Y, Döring M, Ower G, Hernández Robles DR, Plata Corredor CA, Stjernegaard Jeppesen T, Örn A, Vandepitte L, Hobern D, Schalk P, DeWalt RE, Ma K, Miller J, Orrell T, Aalbu R, Abbott J, Adlard R, Aedo C, et al. (Eds) Catalogue of Life Checklist. https://doi.org/10.48580/dfqf-3gk

Nguyen LT, Schmidt HA, von Haeseler A, Minh BQ (2015) IQ-TREE: A fast and effective stochastic algorithm for estimating maximum likelihood phylogenies. Molecular Biology and Evolution 32: 268–274. https://doi.org/10.1093/molbev/msu300

Nixon KC (1999) WINCLADA (Beta), v. 1.00.08. Software published by the author, Ithaca, New York. http://www.Cladistics.com

QGIS Development Team (2020) QGIS Geographic Information System. Open Source Geospatial Foundation Project. Available from: http://qgis.osgeo.org

Rambaut A (2024) FigTree: Tree Figure Drawing Tool. Ver. 1.4.5_pre-release. Available at https://github.com/rambaut/figtree/releases [verified 2 Dec 2024].

Rambaut A, Suchard MA, Xie D, Drummond AJ (2014) Tracer ver. 1.7.1 Available at https://github.com/beast-dev/tracer/releases/tag/v1.7.1 [verified 28 Nov 2021].

Ramírez-Salamanca JM, Cornejo P, Chani-Posse MR (2024) Early evolution of the megadiverse subtribe Philonthina (Staphylinidae: Staphylininae: Staphylinini) and its Neotropical lineage. Systematic Entomology 49(1): 28–47. https://doi.org/10.1111/syen.12605

Ramírez-Salamanca JM, Silva-Tavera DF, Chani-Posse MR (2020) Systematic revision and phylogenetic assessment of two new Neotropical genera of the rove-beetle subtribe Philonthina (Coleoptera: Staphylinidae): *Inesius* gen. nov. and *Rhaegalius* gen. nov**.** Zoologischer Anzeiger 288: 151–167. https://doi.org/10.1016/j.jcz.2020.07.001

Rodríguez-Melgarejo ME, Chani-Posse M (2021) On the rare Neotropical genus *Ophionthus* Bernhauer (Coleoptera: Staphylinidae: Staphylininae): redescription of the type species and description of a new species. European Journal of Taxonomy 735(1): 15–33. https://doi.org/10.5852/ejt.2021.735.1237

Rodríguez-Melgarejo ME, Chani-Posse M (2024) Two new species of the Andean genera *Leptopeltus* Bernhauer and *Leptopeltoides* Chani-Posse & Asenjo (Coleoptera: Staphylinidae: Staphylininae) from the tropical Andes, with a new country record and an updated phylogeny. Zootaxa 5501(2): 345–357. https://doi.org/10.11646/zootaxa.5501.2.7

Rodríguez-Melgarejo ME, Ramírez-Salamanca JM, Chani-Posse MR (submitted) Integrative systematics reveals new brachypterous genera and sheds light on hind wing evolution in the Neotropical lineage of Philonthina (Coleoptera: Staphylinidae). Invertebrate Systematics.

Ronquist F, Teslenko M, van der Mark P, Ayres DL, Darling A, Höhna S, Larget B, Liu L, Suchard MA, Huelsenbeck JP (2012) MrBayes 3.2: efficient Bayesian phylogenetic inference and model choice across a large model space. Systematic Biology 61: 539–542. https://doi.org/10.1093/sysbio/sys029

Scheerpeltz O (1933) Staphylinidae VII. In: Schenkling S (Ed.) Coleopterorum Catalogus 129: 989–1500. W. Junk, Berlin.

Smetana A (1982) Revision of the subfamily Xantholininae of America North of Mexico (Coleoptera: Staphylinidae). Memoirs of the Entomological Society of Canada 12: 1–389. https://doi.org/10.4039/entm114120fv

Smetana A (1995) Rove beetles of the subtribe Philonthina of America north of Mexico (Coleoptera: Staphylinidae): Classification, phylogeny and taxonomic revision. Memoirs on Entomology International 3: 1–946.

Spiessberger EL., Newton AF, Thayer MK, Betz O (2024) Comparative morphology of the feeding apparatus of Staphylinine beetles (Coleoptera: Staphylinidae). Arthropod Systematics and Phylogeny 82: 267–303. https://doi.org/10.3897/asp.82.e114508

Supplementary Material 1

File S1

Authors: Chani-Posse MR, Rodríguez-Melgarejo ME, Ramírez-Salamanca JM (2025)
Data type: .nex
Explanation notes: Morphological matrix (Mesquite).
Copyright notice: This dataset is made available under the Open Database License (http://opendatacommons.org/licenses/odbl/1.0). The Open Database License (ODbL) is a license agreement intended to allow users to freely share, modify, and use this dataset while maintaining this same freedom for others, provided that the original source and author(s) are credited.
Link: https://doi.org/10.3897/asp.83.e150304.suppl1

ZOBODAT - www.zobodat.at

Zoologisch-Botanische Datenbank/Zoological-Botanical Database

Digitale Literatur/Digital Literature

Zeitschrift/Journal: Arthropod Systematics and Phylogeny

Jahr/Year: 2025

Band/Volume: 83

Autor(en)/Author(s): Chani-Posse Mariana, Rodriguez-Melgarejo Maryzender, Ramirez-Salamanca Jose Manuel

Artikel/Article: Systematics and phylogeny of the Andean genera Konradus Chani-Posse & Ramírez-Salamanca and Yuracarus gen. nov. (Coleoptera: Staphylinidae) 331-352